© 2015. Published by The Company of Biologists Ltd | Development (2015) 142, 871-882 doi:10.1242/dev.110759

RESEARCH ARTICLE

STEM CELLS AND REGENERATION

Hnf1b controls pancreas morphogenesis and the generation of Ngn3+ endocrine progenitors

Matias G. De Vas[1,2,3], Janel L. Kopp[4], Claire Heliot[1,2,3], Maike Sander[4], Silvia Cereghini[1,2,3] and Cécile Haumaitre[1,2,3,*]

ABSTRACT

Heterozygous mutations in the human *HNF1B* gene are associated with maturity-onset diabetes of the young type 5 (MODY5) and pancreas hypoplasia. In mouse, *Hnf1b* heterozygous mutants do not exhibit any phenotype, whereas the homozygous deletion in the entire epiblast leads to pancreas agenesis associated with abnormal gut regionalization. Here, we examine the specific role of *Hnf1b* during pancreas development, using constitutive and inducible conditional inactivation approaches at key developmental stages. *Hnf1b* early deletion leads to a reduced pool of pancreatic multipotent progenitor cells (MPCs) due to decreased proliferation and increased apoptosis. Lack of Hnf1b either during the first or the secondary transitions is associated with cystic ducts. Ductal cells exhibit aberrant polarity and decreased expression of several cystic disease genes, some of which we identified as novel Hnf1b targets. Notably, we show that Glis3, a transcription factor involved in duct morphogenesis and endocrine cell development, is downstream Hnf1b. In addition, a loss and abnormal differentiation of acinar cells are observed. Strikingly, inactivation of *Hnf1b* at different time points results in the absence of Ngn3$^+$ endocrine precursors throughout embryogenesis. We further show that Hnf1b occupies novel *Ngn3* putative regulatory sequences *in vivo*. Thus, Hnf1b plays a crucial role in the regulatory networks that control pancreatic MPC expansion, acinar cell identity, duct morphogenesis and generation of endocrine precursors. Our results uncover an unappreciated requirement of Hnf1b in endocrine cell specification and suggest a mechanistic explanation of diabetes onset in individuals with MODY5.

KEY WORDS: Hnf1b, Pancreas, MODY5, Progenitors, Cystic ducts, Ngn3, Mouse, Human

INTRODUCTION

The pancreas is an abdominal gland that is essential for nutrient homeostasis formed by acinar, ductal and endocrine cells. Acinar cells, organized in acini, secrete digestive enzymes into the duodenum via the ductal network. Endocrine cells are organized in the islets of Langerhans, notably composed of α, β and δ cells, which secrete the hormones glucagon, insulin and somatostatin, respectively. In mice, the pancreas is specified by embryonic day (E) 8.5. Early pancreas morphogenesis, known as the primary transition, is characterized by active proliferation of epithelial multipotent progenitor cells (MPCs), followed by a period of growth and differentiation from E12.5, called the secondary transition, to form acinar, ductal and endocrine cells. Regionalization of the early epithelium results in a pre-acinar domain in the tips of the branching organ and a central bipotential ductal/endocrine trunk domain, from which endocrine cells differentiate (Seymour and Sander, 2011). Notch signaling plays an important role in this process (Afelik and Jensen, 2013). Numerous transcription factors have been implicated in the regulation of pancreas development (Pan and Wright, 2011). Foxa1/a2 are dominant regulators of *Pdx1* expression (Gao et al., 2008). *Pdx1* and *Ptf1a* determine fate specification of pancreatic MPCs (Pan and Wright, 2011), whereas *Sox9* maintains MPCs, by preventing apoptosis and promoting proliferation (Seymour et al., 2007). *Ngn3* is required for endocrine cell differentiation (Gradwohl et al., 2000). During the secondary transition, *Sox9* and *Hnf6* are both expressed in the bipotent duct/endocrine domain and required for maintaining *Ngn3* expression (Dubois et al., 2011; Jacquemin et al., 2000; Seymour et al., 2008). After the secondary transition, endocrine and exocrine cell populations expand and differentiate to generate the mature hormone- and enzyme-producing cell types of islets and acini, respectively.

Among transcription factors, hepatocyte nuclear factor 1b (Hnf1b) is expressed in the pre-pancreatic foregut endoderm and in pancreatic MPCs. A sequential transcriptional cascade of *Hnf1b→Hnf6→Pdx1* was found to direct differentiation of endodermal cells into pancreatic progenitors (Poll et al., 2006). From ∼E14.5 to adulthood, Hnf1b expression is restricted to the embryonic ductal cords that later form the adult ductal cells (Haumaitre et al., 2005; Kopp et al., 2011; Maestro et al., 2003; Nammo et al., 2008). We have previously shown that *Hnf1b*-deficient mouse embryos rescued by tetraploid aggregation exhibit pancreas agenesis, with a transient dorsal bud expressing Pdx1 but not Ptf1a, showing that Hnf1b is required for pancreas specification (Haumaitre et al., 2005). Regionalization of the gut was also affected, as revealed by ectopic expression of *Shh*, which could contribute to reduce the Pdx1$^+$ pre-pancreatic domain. *Hnf1b*-deficient embryos also exhibit impaired specification of other organs derived from the ventral endoderm, including liver (Lokmane et al., 2008). Thus, it was difficult to distinguish the role of *Hnf1b* in the pancreas from its role in regionalizing the primitive intestine. Moreover, the severity of the phenotype precluded the analysis of crucial later roles of Hnf1b during pancreas differentiation. Indeed, lineage-tracing analyses revealed that embryonic Hnf1b$^+$ cells of the branching pancreas are precursors of acinar, duct and endocrine lineages (Solar et al., 2009). In humans, *HNF1B* heterozygous mutations are associated with 'maturity onset diabetes of the young type 5' (MODY5) syndrome, which is characterized by early onset of diabetes, pancreas hypoplasia and multicystic kidney dysplasia (Bellanné-Chantelot et al., 2004; Chen et al., 2010; Edghill et al., 2006;

[1]CNRS, UMR7622, Institut de Biologie Paris-Seine (IBPS), Paris F-75005, France. [2]Sorbonne Universités, UPMC Université Paris 06, UMR7622-IBPS, Paris F-75005, France. [3]INSERM U969, Paris F-75005, France. [4]Department of Pediatrics and Cellular & Molecular Medicine, Pediatric Diabetes Research Center, University of California-San Diego, La Jolla, CA 92093-0695, USA.

*Author for correspondence (cecile.haumaitre@inserm.fr)

Received 3 April 2014; Accepted 5 January 2015

Development (2015) 142, 871-882 doi:10.1242/dev.110759

Haldorsen et al., 2008). The identification of two fetuses carrying distinct *HNF1B* mutations, associated with polycystic kidneys and severe pancreatic hypoplasia (Haumaitre et al., 2006), further suggested an early developmental role of HNF1B in human pancreas, which might be an important cause of MODY5.

In order to elucidate the specific role of *Hnf1b* in pancreas development, we conditionally inactivated *Hnf1b* in pancreatic MPCs and at later stages. Combined early and late deletion analyses demonstrate the crucial function of Hnf1b in the regulatory networks controlling pancreatic MPC expansion, duct morphogenesis, acinar cell identity and generation of endocrine precursors.

RESULTS

Hnf1b deficiency in pancreatic progenitors leads to severe pancreatic hypoplasia and perinatal lethality

We performed a conditional deletion of *Hnf1b* in pancreatic MPCs using a *Hnf1b*-floxed mouse line (Heliot et al., 2013) crossed with the *Pdx1-Cre* (Wells et al., 2007) or the tamoxifen (TM)-inducible *Sox9-CreER*^{T2} line (Kopp et al., 2011), as *Pdx1* and *Sox9* share a common expression domain with *Hnf1b* in the early pancreas (Dubois et al., 2011; Maestro et al., 2003; Seymour et al., 2007). *Pdx1-Cre;Hnf1b*$^{+/LacZ}$ and *Hnf1b*$^{Flox/Flox}$ mice were crossed to generate *Pdx1-Cre;Hnf1b*$^{Flox/LacZ}$ embryos, referred to as mutants. *Hnf1b*$^{Flox/LacZ}$ and *Hnf1b*$^{+/Flox}$ embryos without the *Pdx1-Cre* transgene were referred to as controls, as haploinsufficient embryos with the *LacZ*-null *Hnf1b* allele did not show any phenotype (Barbacci et al., 1999; Kornfeld et al., 2013). Heterozygous *Pdx1-Cre;Hnf1b*$^{+/Flox}$ embryos also showed no phenotype (Fig. 1E; supplementary material Fig. S1). By contrast, *Pdx1-Cre;Hnf1b*$^{Flox/LacZ}$ mutant embryos displayed severe pancreatic hypoplasia at E18.5 (Fig. 1A-D), corresponding to a 45% and 90% decrease in pancreatic weight at E16.5 and E18.5, respectively (Fig. 1E). We also generated *Pdx1-Cre;Hnf1b*$^{Flox/LacZ}$*;R26R*$^{+/YFP}$ mutants and observed uniform YFP labeling in the remnant pancreatic epithelium, revealing the high efficiency of the *Pdx1*-driven Cre recombination (Fig. 1C′,D′). Hnf1b/GFP co-immunostainings at E10.5 confirmed the extensive deletion of *Hnf1b* in mutants, showing only 16% of remaining Hnf1b^{+}/GFP^{-} cells due to a slight mosaic expression of the *Pdx1-Cre* line (Fig. 1F-G′). In accordance, we found a 70% decrease in wild-type (WT) *Hnf1b* transcripts at E12.5 (Fig. 1H). Histological analysis by Hematoxylin and Eosin staining revealed a severe decrease in acinar cells with dispersed clusters of acini, cystic ducts and an apparent absence of endocrine islets in mutant pancreata at E16.5 and E18.5 (Fig. 1I-L). This phenotype was associated with high lethality of mutant pups, as 70% died during the first week of life (Fig. 1M). Interestingly, we found that mutant newborns were hypoglycemic, with a 30% decrease of blood glucose (Fig. 1O). This phenotype correlates with a 93% decrease in glucagon-expressing cells (see Fig. 7O). Hypoglycemia is likely the main cause of mutant lethality at P0/P1 (40%), because immediately after birth, glycogenolysis stimulated by glucagon allows mobilisation of hepatic glycogen, which is the only energetic source available at this stage. *Hnf3a*$^{-/-}$ mice also die perinatally of hypoglycemia, associated with a 50% decrease in glucagon (Kaestner et al., 1999; Shih et al., 1999). By contrast, at P2, mutants became hyperglycemic, with a 44% increase of blood glucose (Fig. 1O), in correlation with the 93% decrease in insulin-expressing cells (see Fig. 7O). Furthermore, we found a massive increase of blood amylase in mutants (250%) (Fig. 1P), as is the case in pancreatitis. This was associated with acinar cell defects (see Fig. 4) and a 32% decrease in mutant body weight at P2 (Fig. 1N). This suggests that mutant lethality after P2 may be due to hyperglycemia and to chronic malabsorption.

We also conditionally inactivated *Hnf1b* with the *Sox9-CreER*^{T2} line. Pregnant females from crosses between *Hnf1b*$^{Flox/Flox}$ and *Sox9-CreER*^{T2}*;Hnf1b*$^{+/LacZ}$ mice were injected with TM at E9.5 (Kopp et al., 2011). *Sox9-CreER*^{T2}*;Hnf1b*$^{Flox/LacZ}$ mutants exhibited strong pancreatic hypoplasia at E18.5 (supplementary material Fig. S2A,B), corresponding to a 40% decrease in pancreas weight at E16.5 (supplementary material Fig. S2G). Hematoxylin and Eosin staining of mutant pancreata showed cystic ducts with a severe decrease in acinar cells and absence of islet structures (supplementary material Fig. S2C-F). Efficient *Sox9*-driven Cre recombination was observed with a 70% decrease in *Hnf1b* transcripts at E14.5 (supplementary material Fig. S2H), and further confirmed by Hnf1b and GFP co-immunostainings at E11.5 in *Sox9-CreER*^{T2}*;Hnf1b*$^{Flox/LacZ}$*;R26R*$^{+/YFP}$ mutants (supplementary material Fig. S2I-J′). These data strongly corroborate the findings obtained with the *Pdx1-Cre* line. Therefore, *Hnf1b* inactivation in MPCs leads to severe pancreatic hypoplasia, associated with cystic ducts, a decrease in acinar cells and absence of endocrine cells.

Hnf1b is required for proliferation and survival of MPCs

To investigate the underlying cause of pancreatic hypoplasia in *Pdx1-Cre;Hnf1b*$^{Flox/LacZ}$ mutants, we analyzed the pool of MPCs at E12.5 using Pdx1 immunostaining and observed a 35% decrease in Pdx1^{+} progenitor cells (Fig. 2A). We further analyzed proliferation and apoptosis. We quantified the percentage of mitotic and apoptotic Pdx1^{+} cells using phospho-histone H3 (PHH3) and TUNEL assay, respectively. A 20% decrease in Pdx1^{+} cell proliferation (Fig. 2B,D,E), as well as an 11-fold increase in Pdx1^{+} cell apoptosis (Fig. 2C,F,G) were observed in mutants compared with controls. Thus, both decreased proliferation and increased cell death contribute to the reduction of MPCs in mutants.

Activation of the fibroblast growth factor (FGF) pathway via binding of mesenchymal FGFs to epithelial FGF receptors (FGFRs) is fundamental to promote proliferation of early pancreatic MPCs, especially through the Fgf10/Fgfr2b pathway (Bhushan et al., 2001; Hart et al., 2003; Pulkkinen et al., 2003). Surprisingly, we observed no difference in *Fgfr2b* expression in *Pdx1-Cre;Hnf1b*$^{Flox/LacZ}$ mutants at E12.5, but we found a 70% decrease in *Fgfr4* expression by qRT-PCR (Fig. 2H). Moreover, by *in vivo* chromatin immunoprecipitation (ChIP) on E12.5 pancreata (Fig. 2I), we found Hnf1b bound to a region containing two previously described Hnf1 DNA-binding sites (Shah et al., 2002), at +280 and +355 bp downstream of the *Fgfr4* transcription start site (TSS) in its first intron. These data suggest that modulation of FGF signaling through direct regulation of *Fgfr4 by* Hnf1b may sustain MPC expansion.

The Notch signaling pathway also plays an important role in the maintenance, proliferation and differentiation of pancreatic MPCs (Apelqvist et al., 1999; Hald et al., 2003; Jensen et al., 2000; Murtaugh et al., 2003). In *Pdx1-Cre;Hnf1b*$^{Flox/LacZ}$ pancreata, we observed a downregulation of the Notch ligand *Dll1* (40%), and an upregulation of the effectors *Hey1*, *Hey2* and *Heyl* at E12.5 (Fig. 3A). Interestingly, we found that expression of *Hey* and other Notch members, such as *Notch2* and *Jag1*, remained abnormally high in mutant pancreata at E14.5 contrary to controls, in which these genes are downregulated at this stage (Fig. 3B). Thus, lack of Hnf1b is associated with deregulation of some Notch pathway components. These findings show that *Hnf1b* is essential for proliferation and maintenance of MPCs, at least in part through modulation of FGF and Notch pathways.

Development (2015) 142, 871-882 doi:10.1242/dev.110759

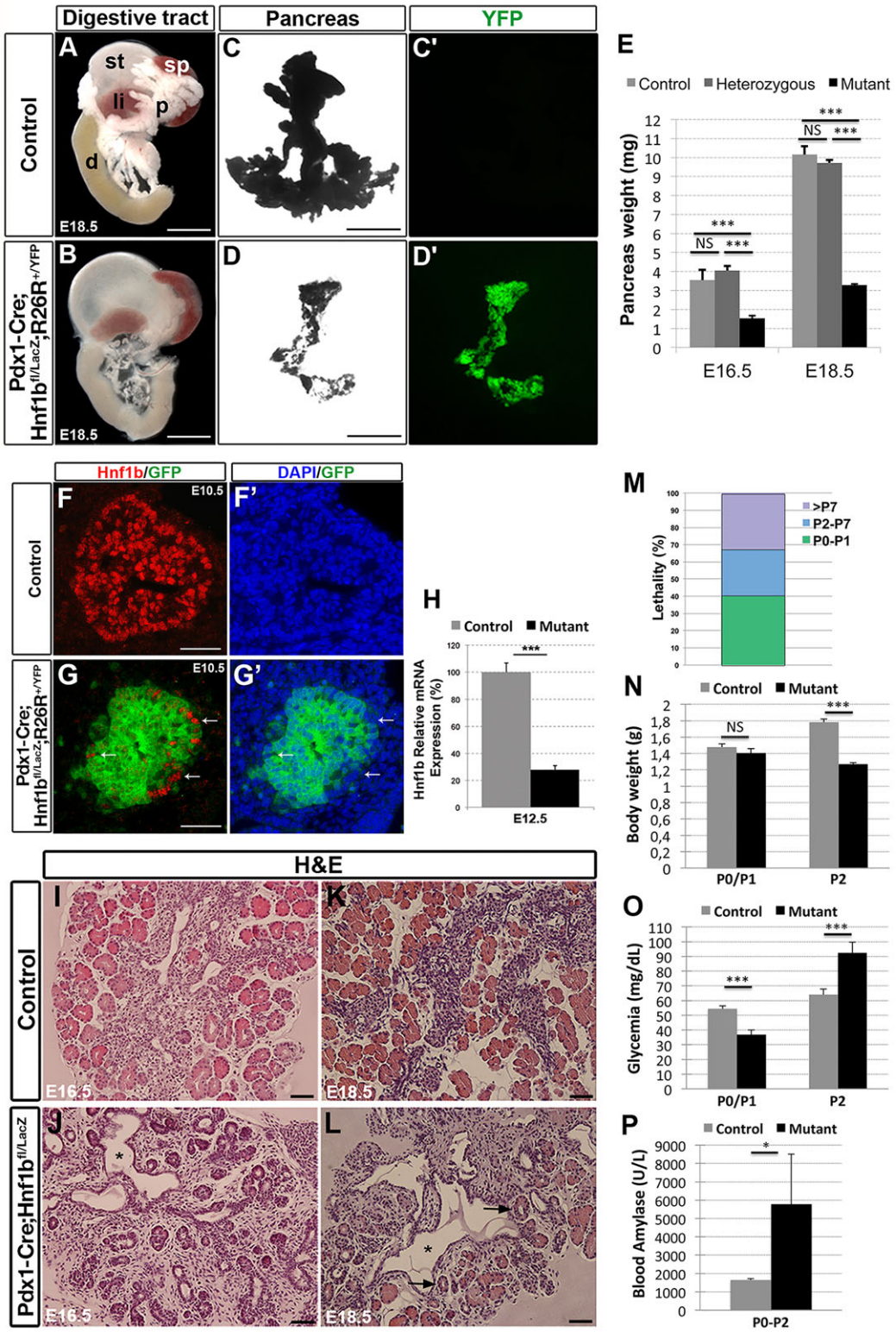

Fig. 1. *Hnf1b* inactivation in pancreatic MPCs leads to a strong pancreas hypoplasia. (A,B) Digestive tracts at E18.5. p, pancreas; st, stomach; sp, spleen; d, duodenum; li, liver. (C,D) E18.5 dissected pancreata. (C′,D′) Recombination shown by the YFP^{+} signal (green) in the *Pdx1-Cre;Hnf1b$^{Flox/LacZ}$;R26R$^{+/YFP}$* mutant pancreas. (E) Pancreas weight at E16.5 and E18.5 in controls, heterozygous (*Pdx1-Cre;Hnf1b$^{Flox/+}$*) and mutants (*Pdx1-Cre;Hnf1b$^{Flox/LacZ}$*) (E16.5: control *n*=9, heterozygous *n*=7, mutant *n*=9; E18.5: control *n*=9, heterozygous *n*=6, mutant *n*=5). (F,G) *Hnf1b* inactivation efficiency in *Pdx1-Cre;Hnf1b$^{Flox/LacZ}$;R26R$^{+/YFP}$* mutant pancreata at E10.5. Hnf1b (red) and GFP (green) co-immunostaining. (F′,G′) Same section showing GFP staining (green) and nuclei stained with DAPI (blue). Only a few Hnf1b^{+} cells are observed in the mutants, which are GFP^{-} (arrows in G,G′). (H) qRT-PCR of wild-type *Hnf1b* transcripts from E12.5 control and *Pdx1-Cre;Hnf1b$^{Flox/LacZ}$* mutant pancreata (control, *n*=6; mutant, *n*=4; *n* being a pool of three pancreata). (I-L) Hematoxylin/Eosin staining of pancreata at E16.5 and E18.5. Asterisks indicate cystic ducts and arrows indicate enlarged acinar lumen in mutants. (M) Lethality of *Hnf1b* mutant mice. (No lethality was observed for control mice.) (N,O) Body weight and glycemia of P0/P1 (control *n*=16, mutant *n*=8) and P2 pups (control *n*=5, mutant *n*=3). (P) Blood amylase in pups (P0-P2: control *n*=15, mutant *n*=5). **P*<0.05; ****P*<0.001. Scale bars: 200 µm in A-D; 50 µm in F,G and I-L.

Development (2015) 142, 871-882 doi:10.1242/dev.110759

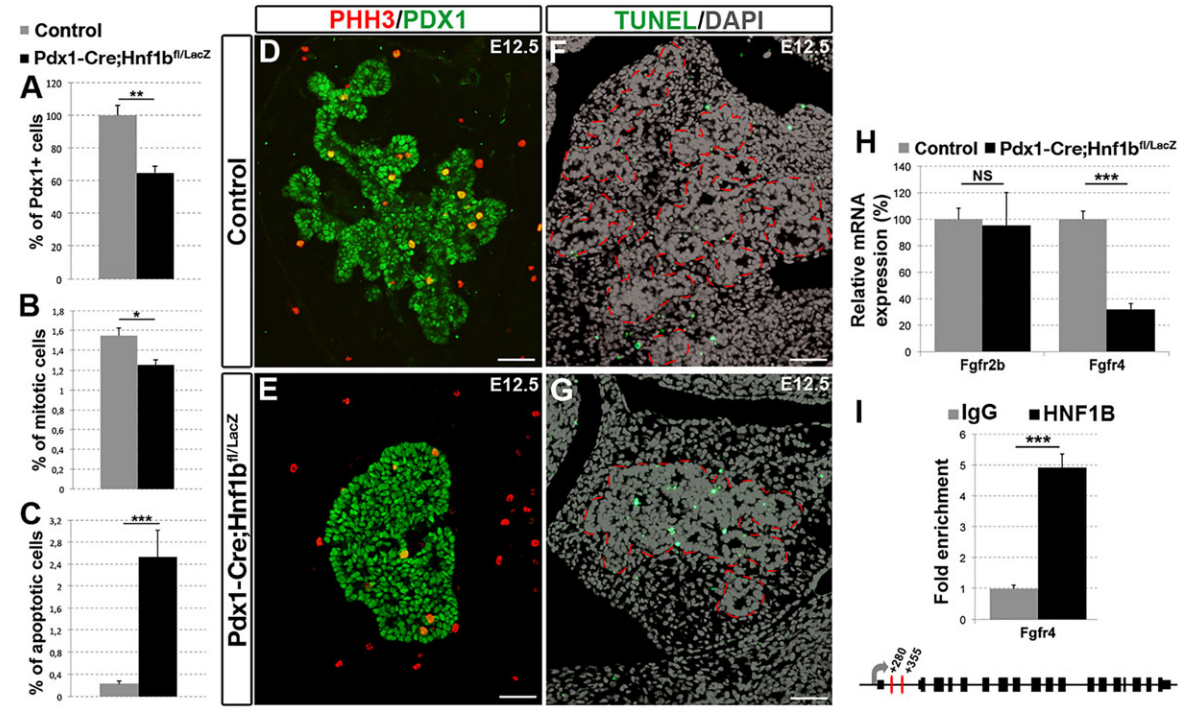

Fig. 2. Hnf1b is required for proliferation and survival of pancreatic MPCs. (A) Percentage of Pdx1^{+} progenitors in control and *Pdx1-Cre;Hnf1b*$^{Flox/LacZ}$ pancreata at E12.5. (B,C) Proliferation and apoptosis of Pdx1^{+} progenitors at E12.5. (D,E) Phospho-histone H3 (PHH3) (red) and Pdx1 (green) immunostaining. (F,G) TUNEL assay (green). The epithelium is encircled in red. Scale bars: 50 µm. (H) qRT-PCR of *Fgfr2b* and *Fgfr4* on E12.5 pancreata. (I) ChIP showing Hnf1b fold enrichment in regulatory regions of *Fgfr4* from E12.5 pancreata immunoprecipitated with an Hnf1b antibody versus control IgG. Hnf1-binding sites are shown in red with their positions relative to *Fgfr4* TSS. **P*<0.05; ***P*<0.005; ****P*<0.001.

Lack of Hnf1b leads to acinar cell differentiation defects

The severe loss of acinar cells and the impaired architecture of remaining acini with enlarged acinar lumens observed by Hematoxylin and Eosin staining in mutants (Fig 1I-L) led us to investigate acinar defects. Amylase immunostaining (Fig. 4A-H) and amylase^{+} cross-sectional area quantification at E16.5 showed a 20% decrease in acinar area in *Pdx1-Cre;Hnf1b*$^{Flox/LacZ}$ mutants (Fig. 4J). A 67% decrease in *Amylase* expression was observed at E16.5 by qRT-PCR (Fig. 4I), suggesting that *Amylase* expression might be reduced in the remaining mutant acinar cells. We also found an eightfold increase of apoptotic mutant acinar cells (Fig. 4L), which cannot be fully compensated for by a twofold increase of mitotic acinar cells (Fig. 4K). In addition, we analyzed expression of the early acinar markers *Ptf1a*, *Mist1* (*Bhlha15* – Mouse Genome Informatics) and *Nr5a2* (Hale et al., 2014; Pin et al., 2001). Expression of *Mist1* was severely reduced before and during the onset of acinar differentiation, with a 50% and an 80% decrease at E12.5 and E14.5, respectively (Fig. 4I). We also observed a 64% decrease of *Ptf1a* at E14.5 and a 35% decrease of *Nr5a2* at E16.5 (Fig. 4I). Notably, an equivalent severe decrease in acinar cells was found in *Sox9-CreER*^{T2}*;Hnf1b*$^{Flox/LacZ}$ (TM E9.5), with a 74% downregulation of amylase gene expression at E16.5 (supplementary material Fig. S3E).

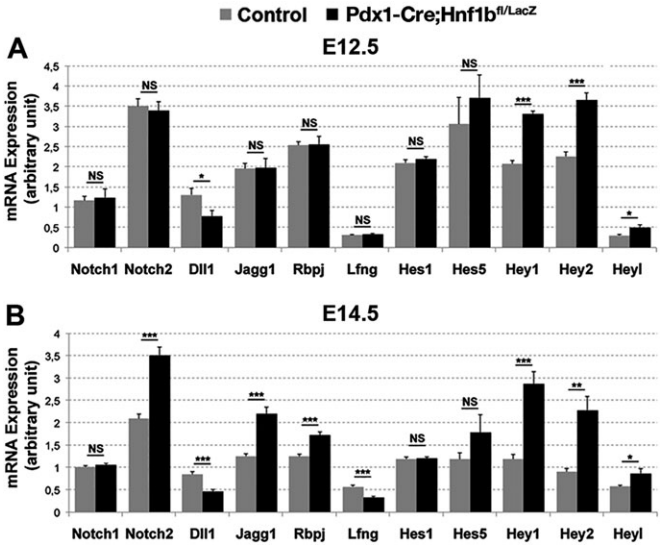

Fig. 3. Lack of Hnf1b is associated with a deregulated Notch pathway. (A,B) qRT-PCR analysis of Notch pathway genes in control and *Pdx1-Cre;Hnf1b*$^{Flox/LacZ}$ pancreata at E12.5 (A) and at E14.5 (B) (control, *n*=7; mutant, *n*=8). *Dll1* is downregulated and Hey factors are upregulated at E12.5; high expression of *Notch2*, *Jag1*, *Rbpj*, *Hey1* and *Hey2* is maintained in mutants at E14.5. **P*<0.05; ***P*<0.005; ****P*<0.001.

Interestingly, the ductal marker Hnf6 was almost undetectable in *Pdx1-Cre;Hnf1b*$^{Flox/LacZ}$ pancreatic ducts, but was found to be ectopically expressed in some differentiated acinar cells at E16.5 (Fig. 4A-D). Ectopic expression of another ductal marker, Sox9, was also observed in mutant acini (Fig. 5C,D). This was accompanied by expanded expression of the ductal marker cytokeratin (pan-CK) (Fig. 4E-H) and by a twofold upregulation of *Ck19* observed by qRT-PCR (Fig. 4I). In agreement with these observations, the Sox9^{+} cross-sectional area increased threefold in mutant pancreata (Fig. 4J), even though the proliferation rate in this compartment was not significantly changed (Fig. 4K).

Thus, lack of Hnf1b leads to increased acinar cell death and reduced expression of acinar cell markers, accompanied by ectopic

Development (2015) 142, 871-882 doi:10.1242/dev.110759

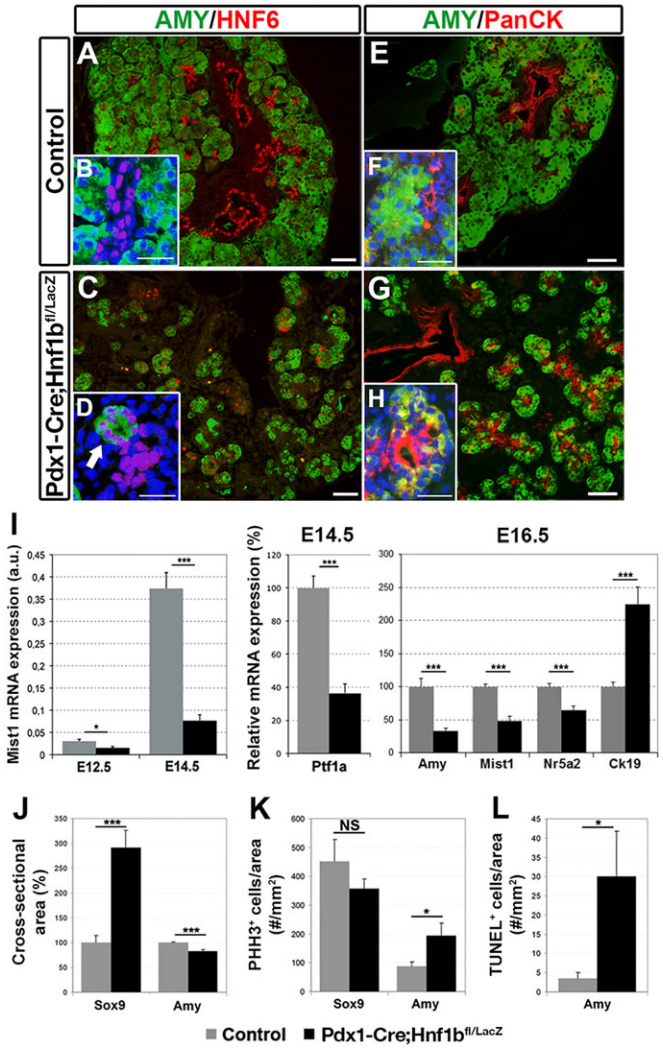

Fig. 4. Lack of Hnf1b leads to acinar cell differentiation defects. (A-D) Amylase (green) and Hnf6 (red) immunostaining in control and *Pdx1-Cre;Hnf1b*$^{Flox/LacZ}$ pancreata at E16.5. (A,B) Hnf6 expression is found in control ducts but not in in acinar amylase^{+} cells. (C,D) Absence of Hnf6 expression in mutant ducts and ectopic expression of Hnf6 in acinar amylase^{+} cells (arrow in D). Nuclei are stained with DAPI (blue). (E-H) Amylase (green) and pan-cytokeratin (PanCK, red) immunostaining at E16.5. (G,H) Increased cytokeratin expression in intercalated mutant ducts and centro-acinar cells. (I) qRT-PCR of *Mist1*, *Ptf1a*, *Nr5a2*, amylase and *Ck19* at E12.5, E14.5 and E16.5 (control, *n*=11; mutant, *n*=11) (a.u., arbitrary unit). (J) Quantification of ductal Sox9^{+} and acinar amylase^{+} sectional areas. (K) Quantification of Sox9^{+} and amylase^{+} cells in proliferation by PHH3 immunostaining at E16.5. (L) Quantification of amylase^{+} acinar cells in apoptosis by TUNEL assay at E16.5. Scale bars: 50 µm in A,C,E,G; 25 µm in B,D,F,H. **P*<0.05; ****P*<0.001.

expression of ductal markers. These results uncover an early role of Hnf1b in acinar differentiation and maintenance of acinar cell identity.

Hnf1b controls duct morphogenesis by regulating cystic disease-associated genes

We performed Sox9 immunostaining at different stages of pancreas development to further analyze duct morphogenesis (Fig. 5A-F). Cystic ducts at E16.5 in *Pdx1-Cre;Hnf1b*$^{Flox/LacZ}$ mutants showed some multilayered epithelium (Fig. 5B,D). Moreover, lack of Sox9 (Fig. 5E,F) or AQP1 expression (Fig. 5K-L′) revealed loss of ductal cell identity in large cystic ducts. We further analyzed the localization of polarity markers in mutants. Similar to PanCK (Fig. 4E-H), strong and expanded β-catenin expression to basal and apical membranes was observed in terminal enlarged ductal cells (Fig. 5G-H′). The basal expression of dystroglycan (Fig. 5G-H′) and laminin (Fig. 5I-J′) was also disrupted in most mutant acinar cells, further illustrating the defects in acinar cells and acquisition of ductal features. Importantly, although control ducts showed strong apical localization of ezrin, PKCz and MUC1 in epithelial cells around the duct lumen, expression of these apical markers in the cells lining cysts was reduced and discontinuous (Fig. 5M-R′). Cyst formation is often associated with an absence or dysfunction of primary cilia (Ware et al., 2011). Immunostaining of acetylated tubulin, a specific component of the cilium axoneme, revealed that cystic cells were devoid of primary cilia (Fig. 5S,T), whereas cilia were still present in non-cystic ducts, suggesting that Hnf1b is not required for primary cilium formation. Similar cystic ducts were observed in *Sox9-CreER*^{T2}*;Hnf1b*$^{Flox/LacZ}$ (TM E9.5) mutants (supplementary material Fig. S4A,B), with altered ductal cell polarity and abnormal localization of β-catenin (supplementary material Fig. S4C,D). Notably, *Sox9-CreER*^{T2}*;Hnf1b*$^{Flox/LacZ}$ (TM E12.5) mutants also displayed cystic ducts (supplementary material Fig. S5D,E). These data show that Hnf1b is required for morphogenesis and for epithelial polarization of ductal cells.

To gain insight into how Hnf1b controls ductal cell differentiation, we further investigated the expression of cystic disease genes in *Pdx1-Cre;Hnf1b*$^{Flox/LacZ}$ mutants. Although *Hnf1b* and *Sox9* are both expressed in pancreatic ducts, and despite the cystic phenotype of pancreatic *Sox9* mutants (Shih et al., 2012), we found no change in *Sox9* expression in our mutants (Fig. 5U). By contrast, *Hnf6* expression was strongly decreased in mutant ductal cells both by immunostaining (Fig. 4A,C) and by qRT-PCR at E14.5 (Fig. 5U), in line with the cystic phenotype of *Hnf6*$^{-/-}$ pancreata (Pierreux et al., 2006; Zhang et al., 2009). We also observed a decrease in *Spp1* expression, which is directly regulated by *Hnf1b* in renal cells (Senkel et al., 2005). Importantly, we found a 90% downregulation of the autosomal recessive PKD gene *Pkhd1* (Ward et al., 2002), and a dramatic decrease in the expression of the key cystic disease genes *Kif12* (Mrug et al., 2005), *Cys1* (Hou et al., 2002), *Bicc1* (Cogswell et al., 2003; Lemaire et al., 2015) and *Glis3* (Kang et al., 2009b) (Fig. 5U). *Cys1* and *Glis3* are of particular interest. *Cys1* is responsible for congenital polycystic kidney (CPK) disease (Tao et al., 2009) and is involved in ciliogenesis and polarization of cholangiocytes (Raynaud et al., 2011), whereas Glis3 is implicated in polycystic disease in both kidney (Kang et al., 2009a) and pancreas (Kang et al., 2009b). Among these genes, *Kif12*, *Pkhd1*, *Pkd2* and *Bicc1* were identified as direct *Hnf1b* targets in the kidney (Gong et al., 2009; Gresh et al., 2004; Verdeguer et al., 2010). Thus, we analyzed whether *Hnf1b* could be a major regulator of these genes in the pancreas by ChIP experiments on E12.5 pancreata (Fig. 5V). Our results showed that Hnf1b is recruited to Hnf1-binding sites in the first intron of Hnf6, within a region known to drive Hnf6 expression in E8.75 pancreatic endoderm (Poll et al., 2006). Moreover, Hnf1b bound to a region carrying a site in the *Pkhd1* promoter previously identified in the kidney (Gresh et al., 2004). Remarkably, we identified two novel Hnf1b target genes: *Cys1* and *Glis3* (Fig. 5V). These results suggest that Hnf1b is a key regulator of duct morphogenesis, exerting direct control of crucial genes involved in duct morphogenesis and cystogenesis.

Hnf1b expression in ducts controls exocrine morphogenesis

To examine the specific requirement of Hnf1b in the ductal compartment, we inactivated *Hnf1b* at late embryogenesis (~E15),

Development (2015) 142, 871-882 doi:10.1242/dev.110759

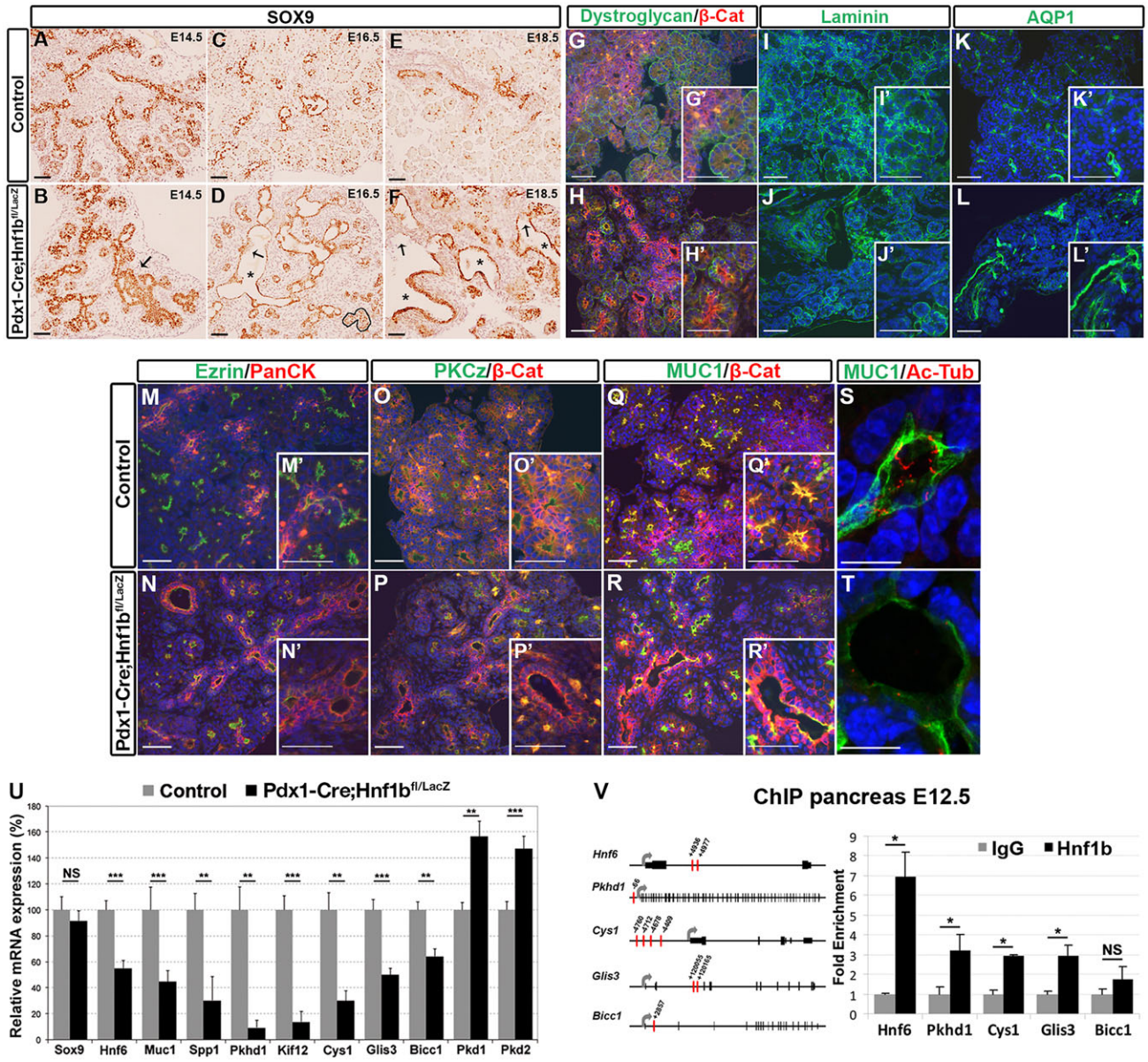

Fig. 5. Hnf1b is crucial for duct morphogenesis. (A-F) Sox9 immunohistochemistry (brown) in control and *Pdx1-Cre;Hnf1b*$^{Flox/LacZ}$ pancreata at E14.5, E16.5 and E18.5. In mutants, note the epithelium multistratified regions at E14.5 (B; arrow), the cystic ducts from E16.5 (D,F; asterisks) with multilayered epithelia (D; arrow), a group of acinar cells ectopically expressing Sox9 (D; encircled in black) and the loss of ductal marker expression at E18.5 (F; arrows). Immunostaining at E16.5 for dystroglycan (green) and β-catenin (β-Cat, red) (G,H); laminin (green) (I,J); AQP1 (green) (K,L); ezrin (green) and PanCK (red) (M,N); PKCz (green) and β-Cat (red) (O,P); mucin 1 (MUC1, green) and β-Cat (red) (Q,R); and MUC1 (green) and acetylated α-Tubulin (Ac-Tub, red) (S,T). There is a strong decrease in dystroglycan and laminin basal marker staining in mutant acinar cells (H′,J′), and increased β-catenin staining in the apical region of acinar cells (H′) and in cystic ducts (R′). Ezrin, PKCz and MUC1 staining shows the loss of polarity of cystic ducts with absence or disruption of the apical staining (N′,P′,R′). Mutant ductal epithelial cells stained with MUC1 are devoid of primary cilia stained for Ac-Tub (T). Nuclei are stained with DAPI (blue). (U) qRT-PCR of ductal and cystic disease genes in E14.5 pancreata (control, *n*=7; mutant, *n*=8). (V) ChIP showing Hnf1b fold-enrichment in regulatory regions of *Hnf6*, *Cys1*, *Pkhd1*, *Glis3* and *Bicc1* from E12.5 pancreata immunoprecipitated with an Hnf1b antibody versus control IgG. A scheme showing Hnf1-binding sites (red), relative to TSS (grey), is presented for each gene.

using the inducible *Sox9-CreER*^{T2} line with TM injection at E14.5. Overall pancreas morphology appeared to be normal in mutants at E18.5, and no change in expression of the ductal marker *Sox9* and the acinar marker amylase were observed (Fig. 6A). However, we observed a dramatic decrease in expression of the cystic disease genes *Pkhd1*, *Kif12*, *Cys1* and *Glis3* (Fig. 6A). We further analyzed *Sox9-CreER*^{T2}*;Hnf1b*$^{Flox/LacZ}$ (TM E14.5) mutant pancreata at postnatal day 8 (P8) and observed a significant reduction in pancreas weight (Fig. 6B). Histological analysis at P8 revealed many cystic ducts associated with a severe loss of acinar cells with enlarged acinar lumen often connected with enlarged terminal ducts (Fig. 6C,D). CPA1 immunostaining confirmed the decrease in the number of acinar cells in mutants (Fig. 6E,F). β-Catenin and MUC1 immunostaining revealed altered polarity of mutant ductal cells (Fig. 6G,H), which were also devoid of primary cilia (Fig. 6I,J). These data reinforce the specific role of *Hnf1b* in the control of duct morphogenesis, and suggest that its function in ducts contributes indirectly to the maintenance of acinar cells.

Development (2015) 142, 871-882 doi:10.1242/dev.110759

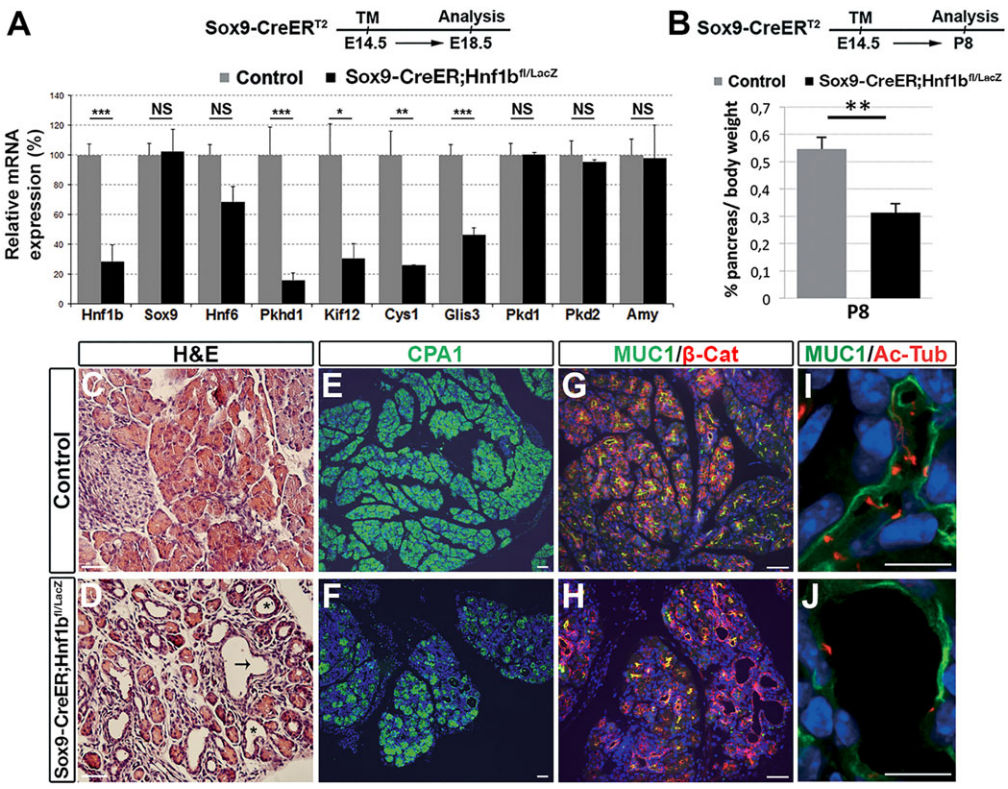

Fig. 6. Hnf1b is required in ducts to maintain the exocrine compartment. (A) *Hnf1b* inactivation in ducts using the Sox9-CreER^{T2} line and TM injection at E14.5. qRT-PCR analysis of control and *Sox9-CreER^{T2};Hnf1b$^{Flox/LacZ}$* (TM E14.5) mutant pancreata at E18.5 (control, *n*=14; mutant, *n*=6). (B) Relative pancreas weight/body weight of animals at P8 (control, *n*=8; mutant, *n*=3). **P*<0.05; ***P*<0.005; ****P*<0.001. (C,D) Hematoxylin/Eosin staining of control and *Sox9-CreER^{T2};Hnf1b$^{Flox/LacZ}$* (TM E14.5) pancreata at P8. Arrow indicates a cystic duct and asterisks indicate dilated terminal ducts. (E,F) Carboxypeptidase (CPA1, green) staining showing fewer acinar cells in mutants. (G,H) MUC1 (green) and β-catenin (red) co-immunostaining shows cystic ducts and loss of polarity. (I,J) MUC1 (green) and Ac-Tub (red) co-immunostaining shows mutant ductal cells devoid of primary cilia. Nuclei are stained with DAPI (blue). Scale bars: 50 µm in C-H; 10 µm in I,J.

Hnf1b controls the generation of Ngn3$^+$ endocrine precursors

As Hnf1b$^+$ cells were defined as immediate precursors of Ngn3$^+$ cells by immunohistochemistry (Maestro et al., 2003; Nammo et al., 2008; Rukstalis and Habener, 2007), and lineage-tracing analyses showed that embryonic Hnf1b$^+$ cells give rise to precursors of endocrine cells (Solar et al., 2009), we analyzed whether *Hnf1b* is required for the generation of these cells. Interestingly, we observed an almost complete loss of Ngn3$^+$ cells (Fig. 7A-F), associated with a 70%, 85% and 93% decrease in *Ngn3* expression observed by qRT-PCR in *Pdx1-Cre;Hnf1b$^{Flox/LacZ}$* pancreata at E12.5, E14.5 and E16.5, respectively (Fig. 7M). Endocrine cell differentiation was almost completely abrogated (Fig. 7G-L), as evidenced by a 93% decrease in insulin$^+$ and glucagon$^+$ areas at E16.5 (Fig. 7O), and decreased transcripts for insulin, glucagon and somatostatin (Fig. 7N). *Sox9-CreER^{T2};Hnf1b$^{Flox/LacZ}$* (TM E9.5) mutants showed a similar dramatic loss of Ngn3$^+$ cells (supplementary material Fig. S3A,B) and an 86% decrease in *Ngn3* expression at E16.5 (supplementary material Fig. S3E). Insulin$^+$ and glucagon$^+$ areas were also severely reduced in size (supplementary material Fig. S3C,D), and insulin, glucagon and somatostatin mRNA levels decreased (supplementary material Fig. S3E).

To determine whether *Hnf1b* specifically controls the generation of endocrine precursors, excluding possible indirect effects due to the early *Hnf1b* deficiency in MPCs, we conditionally inactivated *Hnf1b* in the pancreatic epithelium during the secondary transition at ~E13, when the major wave of endocrine cell neogenesis occurs. The *Hnf1b*-floxed locus was efficiently recombined in *Sox9-CreER^{T2};Hnf1b$^{Flox/LacZ}$* (TM E12.5) pancreata at E16.5, as confirmed by a 75% decrease in *Hnf1b* expression (Fig. 7T). Mutant pancreas morphology and organ size appeared normal, and expression of the acinar markers *Ptf1a*, *Mist1*, *Nr5a2* and amylase were only partially affected at E16.5 (supplementary material Fig. S5A). Strikingly, we found a dramatic loss of Ngn3$^+$ endocrine precursors (Fig. 7P,Q) and a 90% decrease in *Ngn3* expression at E16.5 (Fig. 7T). This coincided with a 81% decrease in insulin$^+$ and a 69% decrease in glucagon$^+$ sectional areas (Fig. 7R,S,U), and downregulation of insulin, glucagon and somatostatin transcripts (Fig. 7T). These results support the specific requirement for *Hnf1b* in the generation of Ngn3$^+$ endocrine progenitors.

These data suggested that Hnf1b directly regulates *Ngn3* expression. We performed ChIP experiments on E12.5 pancreata and found no Hnf1b enrichment −3318 base pairs (bp) upstream *Ngn3* TSS, a region homologous to the human *NGN3* cluster 1 enhancer containing a putative Hnf1-binding site (Lee et al., 2001). Importantly, we found that Hnf1b was recruited to a proximal and a distal region containing Hnf1-binding sites at −697 bp and −4890 bp, respectively (Fig. 7V).These results demonstrate that *Hnf1b* is specifically required to generate endocrine precursors, very likely by directly regulating *Ngn3*.

DISCUSSION

By *Hnf1b* conditional inactivation in the pancreas, our data demonstrate the essential functions exerted by *Hnf1b* in pancreatic MPC expansion and differentiation of exocrine and endocrine lineages, placing this transcription factor in a prominent position in the regulatory networks involved in these processes.

MPCs proliferation and survival

Pancreas hypoplasia observed in *Pdx1-Cre;Hnf1b$^{Flox/LacZ}$* embryos is correlated with a reduced pool of MPCs, as it was previously shown that the progenitor pool defines the final pancreas size (Stanger et al., 2007). *Hnf1b* mutants display similar defects in MPC proliferation to *Gata4/Gata6* compound pancreatic mutants (Xuan et al., 2012), and similar MPC apoptosis to *Sox9* mutants (Seymour et al., 2007). Surprisingly, expression of the key transcription factors

Development (2015) 142, 871-882 doi:10.1242/dev.110759

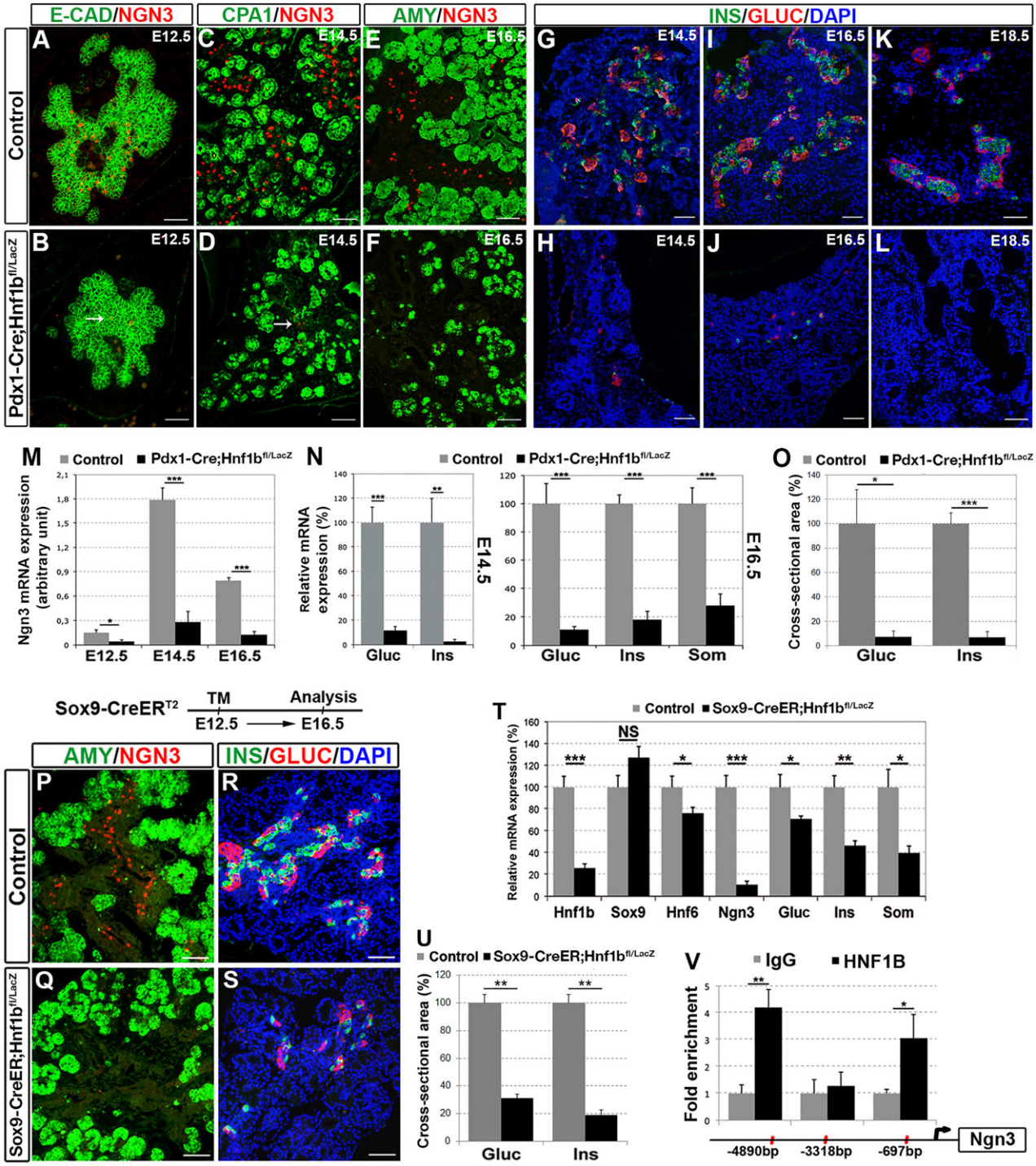

Fig. 7. Hnf1b controls the generation of endocrine precursors through *Ngn3* regulation. (A,B) Immunostaining of Ngn3 (red) and E-Cadherin (E-CAD, green) in control and *Pdx1-Cre;Hnf1b*$^{Flox/LacZ}$ pancreata at E12.5. (C,D) Immunostaining of Ngn3 (red) and CPA1 (green) at E14.5. Arrows indicate a few remaining Ngn3$^+$ cells in mutants (B,D). (E,F) Immunostaining of Ngn3 (red) and amylase (green) at E16.5. (G-L) Immunostaining of insulin (green) and glucagon (red) at E14.5, E16.5 and E18.5. Nuclei are stained with DAPI (blue). (M) qRT-PCR of *Ngn3* at E12.5, E14.5 and E16.5. (N) qRT-PCR of glucagon, insulin and somatostatin at E14.5 and E16.5. (O) Quantification of glucagon$^+$ and insulin$^+$ sectional areas at E16.5. (P-U) *Hnf1b* inactivation during the secondary transition using the Sox9-CreER^{T2} line, with TM injection at E12.5 and analysis at E16.5. (P,Q) Immunostaining of amylase (green) and Ngn3 (red) in *Sox9-CreER*^{T2}*;Hnf1b*$^{Flox/LacZ}$ (TM E12.5) pancreata at E16.5. (R,S) Immunostaining of insulin (green) and glucagon (red). Nuclei are stained with DAPI (blue). (T) qRT-PCR analysis in control and *Sox9-CreER*^{T2}*;Hnf1b*$^{Flox/LacZ}$ (TM E12.5) pancreata at E16.5 (control, *n*=9; mutant, *n*=9). (U) Quantification of glucagon$^+$ and insulin$^+$ sectional areas at E16.5. (V) ChIP showing Hnf1b fold enrichment in regulatory regions of *Ngn3* from E12.5 pancreata immunoprecipitated with an Hnf1b antibody versus control IgG. Hnf1-binding sites are shown in red with their positions relative to the *Ngn3* TSS. **P*<0.05; ***P*<0.005; ****P*<0.001. Scale bars: 50 µm.

Pdx1, *Sox9* and *Ptf1a*, which are involved in MPC expansion (Rieck et al., 2012), was not changed at E12.5 (data not shown), excluding their contribution to the MPC phenotype observed.

We observed that Notch signaling pathway is deregulated in *Hnf1b* mutant pancreata, showing a decrease in *Dll1* expression and upregulation of *Hey* repressors. A direct regulation of *Dll1* by

Development (2015) 142, 871-882 doi:10.1242/dev.110759

Hnf1b, as recently shown in the kidney (Heliot et al., 2013; Massa et al., 2013), does not seem to occur in the pancreas, as ChIP on E12.5 pancreata showed no Hnf1b recruitment to a conserved region of *Dll1* (data not shown). Recent data suggested a role for *Dll1*, which is activated by Ptf1a, in MPC proliferation (Ahnfelt-Ronne et al., 2012). Hes and Hey factors were found to inhibit the activity of the Ptf1 transcriptional complex by direct interaction with Ptf1a, without changing *Ptf1a* mRNA levels (Esni et al., 2004; Ghosh and Leach, 2006). Therefore, in *Hnf1b* mutants, the increased levels of Hey factors observed could inhibit Ptf1 transcriptional complex activity resulting in reduced *Dll1* expression and MPC proliferation.

The reduced proliferation in *Hnf1b*-deficient pancreata could also be attributed to a decreased FGF signaling via downregulation of *Fgfr4*. Although the pancreatic phenotype of *Fgfr4*$^{-/-}$ embryos was not analyzed (Weinstein et al., 1998), several recent studies showed that *Fgfr4* positively regulates proliferation and has anti-apoptotic effects in models of liver, prostate and gastric cancer (Drafahl et al., 2010; Ho et al., 2009; Miura et al., 2012; Ye et al., 2011). Interestingly, both *Fgfr2b* and *Fgfr4* were downregulated in *Sox9*-deficient pancreas (Seymour et al., 2012), raising the possibility that they might serve partially redundant functions in MPC proliferation.

Acinar differentiation and duct morphogenesis

The severe reduction in the number of acinar cells in *Pdx1-Cre; Hnf1b*$^{Flox/LacZ}$ mutants was associated with a differentiation defect and apoptosis. The acinar compartment exhibited ectopic expression of the ductal markers Hnf6 and Sox9, which were shown to be required for acinar metaplasia and repression of acinar genes (Prevot et al., 2012). Moreover, the ductal compartment was increased in size without changing its proliferation rate, suggesting that acini were replaced by the expanded ductal compartment. This acinar defect could be associated with the dramatic decrease in *Mist1* expression, as inhibition of *Mist1* in acinar cells leads to severe defects, including acinar-to-ductal metaplasia (Zhu et al., 2004). The loss of acinar cell identity may also be explained by the previously described link between reduced *Mist1* and *Ptf1a* expression, conversion of acinar cells into ductal cells and upregulation of Notch signaling (Rooman et al., 2006; Rovira et al., 2010; Shi et al., 2009). *Hnf1b* deletion at the onset of acinar cell differentiation (TM at E12.5) also resulted in increased *Hey2* expression, even if less pronounced than in *Pdx1-Cre;Hnf1b*$^{Flox/LacZ}$ mutants, which correlated with downregulation of *Mist1* and *Ptf1a* (supplementary material Fig. S5F), and fewer amylase-expressing cells (supplementary material Fig. S5B,C). These results suggest an early role for Hnf1b in the acquisition of pancreatic acinar cell identity from MPCs, possibly through Mist1, Ptf1a and Hey factors. Later Hnf1b deletion (TM at E14.5) was associated with a defect in acinar cell maintenance. As Hnf1b is not expressed in acinar cells, these late acinar defects might be an indirect consequence of abnormal duct morphogenesis, as described in pancreata deficient for *Jag1* (Golson et al., 2009) or *Kif3a* (Cano et al., 2006).

Our results show that Hnf1b is required for both early and late control of duct morphogenesis; *Hnf1b* deletion resulted in cystic ducts with altered polarity and a lack of primary cilia. Cilia loss in ductal cells is an important event in pancreatic cyst development. However, despite lack of cilia throughout development in *Kif3a* mutants, duct dilatations do not occur before E17.5 (Cano et al., 2006). The pancreatic epithelium in *Hnf1b* mutants is dilated from E14.5, thus indicating that Hnf1b plays additional roles in duct morphogenesis. Conditional *Hnf1b* deletion at late embryogenesis also resulted in a polycystic pancreas postnatally, showing the direct requirement of *Hnf1b* in duct morphogenesis and further suggesting that the cystic phenotype is not a consequence of an early blocked endocrine differentiation (Magenheim et al., 2011). As in *Hnf6*$^{-/-}$ pancreata (Pierreux et al., 2006), cysts in *Hnf1b* mutants were not associated with increased epithelial cell proliferation. In *Hnf6* and *Sox9* mutants, cyst formation also seems to occur by deregulation of cystic-associated genes, but the genes involved are different. *Sox9* mutants were characterized by a decrease in *Pkd2* expression (Shih et al., 2012), whereas *Hnf6* mutants displayed downregulation of *Pkhd1* (Pierreux et al., 2006). We observed a marked decrease in *Hnf6* expression in mutant pancreatic ducts at E14.5 upon deletion in MPCs, which correlated with the finding that Hnf1b is recruited at E12.5 to *Hnf6* regulatory sequences known to drive expression in the pancreatic endoderm (Poll et al., 2006). Similarly, in *Hnf6* mutants, Hnf1b expression is reduced during a narrow time window and then re-induced at late embryogenesis (Pierreux et al., 2006), illustrating the existence of a complex Hnf1b-Hnf6 feed-forward loop involved in duct morphogenesis at least between E12.5 and E16.5. However, duct morphogenetic defects of *Hnf1b* mutants are not simply explained by this transient cross-regulation. Indeed, duct morphogenesis is more largely affected in *Hnf1b* mutants than in *Hnf6* mutants, as cysts affect all types of ducts, and not only intralobular and interlobular ducts, as in *Hnf6* mutants (Pierreux et al., 2006). Moreover, whereas *Glis3* expression was unaffected in *Hnf6*-null pancreas (Kang et al., 2009b), we found that Glis3 is downstream Hnf1b, which is particularly interesting as both factors are associated with cystogenesis (Kang et al., 2009a,b) and endocrine cell development (Kim et al., 2012). Taking advantage of Hnf1b ChIP-seq analysis on embryonic kidneys, we identified *Glis3* and *Cys1* as novel Hnf1b targets in pancreas. *Cys1* was found decreased in *Hnf6* and *Hnf1b* mutant livers, although a direct regulation of *Cys1* by Hnf1b was not established in biliary ducts (Raynaud et al., 2011). These studies show that Hnf1b is an essential regulator of key ductal genes related to cyst development in different organs. However, the regulatory circuits operating in ducts can diverge: *Pkhd1* expression decreases in both pancreas and kidney, but not in the liver of *Hnf1b* mutants; *Pkd2* expression decreases in the kidney, but not in the pancreas of *Hnf1b* mutants (Gresh et al., 2004; Hiesberger et al., 2005; Raynaud et al., 2011). Our study uncovers a crucial transcriptional network in pancreatic ductal cells, in which Hnf1b exerts a prominent role.

Control of endocrine progenitors

We show loss of *Ngn3* expression upon *Hnf1b* inactivation during the first and secondary transitions, as well as the recruitment of Hnf1b to putative regulatory regions of *Ngn3*. This demonstrates an essential role of *Hnf1b* in the specification of endocrine progenitors. Additional transcription factors, including Hnf6, Glis3, Pdx1, Foxa2 and Sox9, were found to directly regulate *Ngn3* expression (Jacquemin et al., 2000; Kim et al., 2012; Oliver-Krasinski et al., 2009; Seymour et al., 2008). Binding sites for some of these factors in the 5′ regulatory region of *Ngn3* are listed in supplementary material Fig. S6. *Hnf6*$^{-/-}$ embryos exhibit markedly reduced numbers of Ngn3^{+} cells at mid-embryogenesis, associated with decreased *Hnf1b* expression (Jacquemin et al., 2000). By E17.5, *Hnf1b* expression is partially restored and reduction of Ngn3^{+} cells is clearly less pronounced when compared with earlier time points, supporting the notion that downregulation of *Hnf1b* in *Hnf6* mutants might be important for *Ngn3* downregulation (Maestro et al., 2003). Pdx1 also contributes to *Ngn3* regulation and, together with Hnf6 (Oliver-Krasinski et al., 2009) and Glis3 (Kim et al., 2012; Yang et al., 2011), occupies an evolutionary conserved enhancer homologous to human cluster 1 (Lee et al., 2001). *Ngn3* cluster 1

Development (2015) 142, 871-882 doi:10.1242/dev.110759

also contains putative Sox9-binding sites (at −3.3 kb), which were occupied by Sox9 in ChIP experiments on mPAC ductal cells (Lynn et al., 2007). However, ChIP on embryonic pancreata demonstrated that Sox9 was not bound to cluster 1, but to three other regions: one distal (at −4.0 kb) and two proximal (at −0.4 kb and −161 bp) (Seymour et al., 2008). Although there is a Hnf1-binding site in the homologous mouse cluster 1, Hnf1b, like Sox9, failed to transactivate this enhancer in transfected HePG2 cells (Oliver-Krasinski et al., 2009), which correlates with our findings showing no Hnf1b recruitment to this region by ChIP. Moreover, Hnf1b did not transactivate the *Ngn3* promoter corresponding to −4864 bp to +88 bp (Ejarque et al., 2013), whereas this factor was able to activate the *Ngn3* full promoter (−5800 to +40 bp) (Yang et al., 2011), suggesting that the Hnf1b-binding site we identified at −4890 bp might be important for *Ngn3* activation. These studies support the existence of distinct enhancer modules with differential binding of essential transcription factors that contribute to the activation of *Ngn3*. Our results show the absolute requirement of Hnf1b for endocrine specification, placing this factor in a prominent position in the regulatory network controlling *Ngn3* expression.

A model depicting *Hnf1b* functions during pancreas development is presented in Fig. 8. As increasing the pool of endocrine progenitors is a key step for the development of cell-based strategies for diabetes, these findings might be of clinical significance to improve *in vitro* protocols for cell-replacement therapies. Proper regulation of *Hnf1b* expression appears to be crucial for endocrine cell formation, and Hnf1b can be used as a marker of progenitor cells with the capacity to robustly produce endocrine cells *in vitro*. In addition, our results suggest that MODY might occur not only as a consequence of β-cell dysfunction, but also as a consequence of defects during development leading to diabetes later in life.

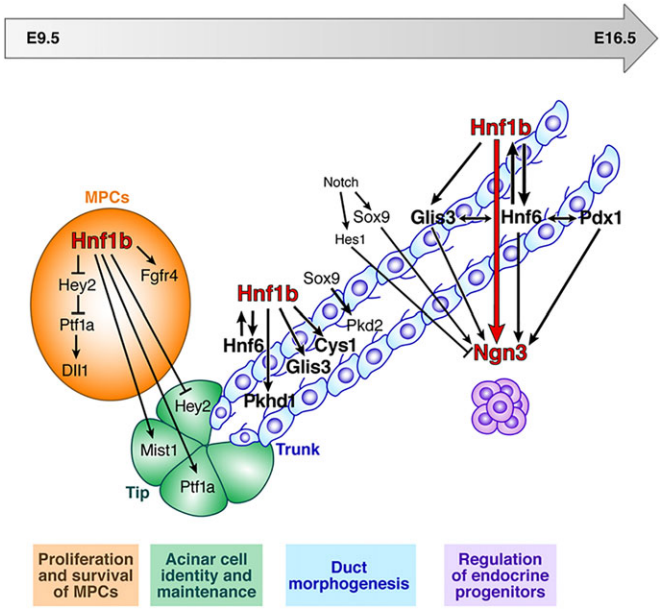

Fig. 8. Proposed model for Hnf1b function in the regulatory networks governing pancreas development. Hnf1b appears to control MPC proliferation and survival by directly regulating Fgfr4 and acting as a negative regulator of the Hey factors, which are inhibitors of the Ptf1a transcriptional complex that in turn activates *Dll1*. Hnf1b indirectly controls acinar cell identity and maintenance, possibly through Mist1, Ptf1a and Hey factors. Subsequently, Hnf1b regulates epithelial duct morphogenesis through the direct control of the key cystic disease genes *Glis3*, *Pkhd1*, *Cys1* and *Hnf6*. Hnf1b is absolutely required for the generation of endocrine progenitors, being an essential transcriptional activator of *Ngn3*. Hnf1b appears also to act directly on *Glis3*, but in parallel with Sox9 and Hes1 in the control of *Ngn3*. Arrows indicate epistatic or direct interactions, and double-headed arrows indicate protein-protein interactions. Double arrows indicate a Hnf1b-Hnf6 cross-regulatory loop between E12.5 and E16.5.

MATERIALS AND METHODS

Mouse transgenic lines and physiological analyses

Mice carrying the *Hnf1b*-null allele (*Hnf1b*^{tmsc1} known as *Hnf1b*$^{+/LacZ}$), with the *LacZ* gene replacing the first exon of *Hnf1b* (Barbacci et al., 1999), were maintained as heterozygotes. The *Hnf1b* conditional knockout (*Hnf1b*^{tm1Ics} denoted as *Hnf1b*$^{Flox/Flox}$) carrying *LoxP* sites flanking exon 4 (Heliot et al., 2013), *Pdx1-Cre* (Wells et al., 2007) and *Sox9-CreER*^{T2} (Kopp et al., 2011) lines have been previously described. The *R26R*^{YFP} line (B6.129X1-*Gt (ROSA)26Sortm1(EYFP)Cos*/J) was from The Jackson Laboratory. 4-Hydroxytamoxifen (Sigma) was dissolved at 10 mg/ml in corn oil/10% ethanol and administrated intraperitoneally to pregnant females at a dose of 2 mg. Blood glucose levels were measured using the OneTouch Vita blood glucose meter (LifeScan), blood amylase using the Reflovet Plus analyzer and pancreatic amylase by reflotron assay (Roche). Animal experiments were conducted in accordance with French and European ethical legal guidelines and the local ethical committee for animal care.

Histology, immunohistochemistry and TUNEL assay

Tissues were fixed, embedded in paraffin, sectioned and analyzed by histology, immunohistochemistry and TUNEL assay as described previously (Haumaitre et al., 2005). Primary and secondary antibodies are listed in supplementary material Table S2. The percentage of Hnf1b^{+} cells was quantified by counting the number of Pdx1^{+} cells that were also Hnf1b^{+}, on at least five sections per pancreas (n=4). Quantification of Pdx1^{+} cells at E12.5 was performed with at least five sections per pancreas (control, n=4; mutant, n=4). More than 10,000 Pdx1^{+} cells were counted for each genotype. Quantification of amylase^{+}, Sox9^{+}, insulin^{+} and glucagon^{+} cell surface was performed using ImageJ software, on at least three sections per pancreas at E16.5 co-immunostained with DAPI (control, n=3; mutant, n=5). Primary cilia were analyzed by confocal microscope (LEICA TSC SPE).

RNA extraction and quantitative PCR

Total RNA from embryonic pancreata was isolated using RNeasy Micro-kit (Qiagen) and reverse transcribed using the superscript II RT First-Strand Synthesis System (Life Technologies). qRT-PCR was performed using the Fast SYBR Green Master Mix (Life Technologies). Primer sequences are provided in supplementary material Table S2. The $2^{-\Delta\Delta Ct}$ method was used to calculate expression levels (Livak and Schmittgen, 2001), normalized to cyclophilin A and relative to wild-type cDNA from E15.5 pancreata. Values are shown as mean+s.e.m. Statistical significance was determined using Student's t-test (NS, not significant; *P<0.05; **P<0.005; ***P<0.001).

Chromatin immunoprecipitation

Chromatin immunoprecipitation (ChIP) experiments were performed as described previously (Heliot and Cereghini, 2012), adapted for E12.5 wild-type pancreata. Immunoprecipitated chromatin were analyzed by qPCR and expressed as fold-enrichment values over IgG control. Primer sequences are provided in supplementary material Table S2. Values are shown as mean+s.e.m. Statistical significance was determined using Student's t-test (NS, not significant; *P<0.05; **P<0.005; ***P<0.001). A detailed protocol is provided in the methods in the supplementary material.

Acknowledgements

We thank C. Wright (Vanderbilt University, TN, USA), P. Jacquemin and F. Lemaigre (De Duve Institute, Belgium), and S. Louvet (UMR7622, France) for antibodies; the Centre d'Expérimentation Fonctionnelle (Faculté de Médecine Pitié-Salpêtrière, France) for blood amylase measures; mouse facilities of the UMR722-IBPS; and S. Gournet for illustration.

Competing interests

The authors declare no competing or financial interests.

Author contributions

M.G.D.V. performed experiments, analyzed data and wrote the manuscript. M.S. and J.L.K. provided the Sox9-CreER^{T2} mouse line, advice on experimental procedures and carefully read the manuscript. C. Heliot performed ChIP-seq experiments. S.C. designed the study, contributed to discussions and revised the manuscript. C. Haumaitre designed the study, performed experiments, analyzed data and wrote the manuscript.

Funding

This work was supported by the European Union's Framework Program 7 (EU-FP7)-Marie Curie Initial Training Network (ITN)-Biology of Liver and Pancreatic Development and Disease (BOLD), by the Centre National de la Recherche Scientifique (CNRS), by the Université Pierre et Marie Curie (UPMC) and by the Institut National de la Santé et de la Recherche Médicale (INSERM) (to S.C. and C. Haumaitre); and by the programme Emergence UPMC and the Société Francophone du Diabète (SFD)-Allocation SFD-Industrie Ypsomed (to C. Haumaitre). M.G.D.V. and C. Heliot were recipients of PhD student fellowships from ITN BOLD and the Fondation pour la Recherche sur le Cancer (ARC), respectively. M.S. is supported by the National Institutes of Health (NIH) – NIDDK [R01-DK078803] and J.L.K. was supported by an Advanced Postdoctoral Fellowship from the Juvenile Diabetes Research Foundation (JDRF). Deposited in PMC for release after 12 months.

Supplementary material

Supplementary material available online at
http://dev.biologists.org/lookup/suppl/doi:10.1242/dev.110759/-/DC1

References

Afelik, S. and Jensen, J. (2013). Notch signaling in the pancreas: patterning and cell fate specification. *Wiley Interdiscip. Rev. Dev. Biol.* **2**, 531-544.

Ahnfelt-Ronne, J., Jorgensen, M. C., Klinck, R., Jensen, J. N., Fuchtbauer, E.-M., Deering, T., MacDonald, R. J., Wright, C. V. E., Madsen, O. D. and Serup, P. (2012). Ptf1a-mediated control of Dll1 reveals an alternative to the lateral inhibition mechanism. *Development* **139**, 33-45.

Apelqvist, A., Li, H., Sommer, L., Beatus, P., Anderson, D. J., Honjo, T., Hrabě de Angelis, M., Lendahl, U. and Edlund, H. (1999). Notch signalling controls pancreatic cell differentiation. *Nature* **400**, 877-881.

Barbacci, E., Reber, M., Ott, M. O., Breillat, C., Huetz, F. and Cereghini, S. (1999). Variant hepatocyte nuclear factor 1 is required for visceral endoderm specification. *Development* **126**, 4795-4805.

Bellanné-Chantelot, C., Chauveau, D., Gautier, J.-F., Dubois-Laforgue, D., Clauin, S., Beaufils, S., Wilhelm, J.-M., Boitard, C., Noël, L.-H., Velho, G. et al. (2004). Clinical spectrum associated with hepatocyte nuclear factor-1beta mutations. *Ann. Intern. Med.* **140**, 510-517.

Bhushan, A., Itoh, N., Kato, S., Thiery, J. P., Czernichow, P., Bellusci, S. and Scharfmann, R. (2001). Fgf10 is essential for maintaining the proliferative capacity of epithelial progenitor cells during early pancreatic organogenesis. *Development* **128**, 5109-5117.

Cano, D. A., Sekine, S. and Hebrok, M. (2006). Primary cilia deletion in pancreatic epithelial cells results in cyst formation and pancreatitis. *Gastroenterology* **131**, 1856-1869.

Chen, Y. Z., Gao, Q., Zhao, X. Z., Chen, Y. Z., Bennett, C. L., Xiong, X. S., Mei, C. L., Shi, Y. Q. and Chen, X. M. (2010). Systematic review of TCF2 anomalies in renal cysts and diabetes syndrome/maturity onset diabetes of the young type 5. *Chin. Med. J.* **123**, 3326-3333.

Cogswell, C., Price, S. J., Hou, X., Guay-Woodford, L. M., Flaherty, L. and Bryda, E. C. (2003). Positional cloning of jcpk/bpk locus of the mouse. *Mamm. Genome* **14**, 242-249.

Drafahl, K. A., McAndrew, C. W., Meyer, A. N., Haas, M. and Donoghue, D. J. (2010). The receptor tyrosine kinase FGFR4 negatively regulates NF-kappaB signaling. *PLoS ONE* **5**, e14412.

Dubois, C. L., Shih, H. P., Seymour, P. A., Patel, N. A., Behrmann, J. M., Ngo, V. and Sander, M. (2011). Sox9-haploinsufficiency causes glucose intolerance in mice. *PLoS ONE* **6**, e23131.

Edghill, E. L., Bingham, C., Slingerland, A. S., Minton, J. A. L., Noordam, C., Ellard, S. and Hattersley, A. T. (2006). Hepatocyte nuclear factor-1 beta mutations cause neonatal diabetes and intrauterine growth retardation: support for a critical role of HNF-1beta in human pancreatic development. *Diabet. Med.* **23**, 1301-1306.

Ejarque, M., Cervantes, S., Pujadas, G., Tutusaus, A., Sanchez, L. and Gasa, R. (2013). Neurogenin3 cooperates with Foxa2 to autoactivate its own expression. *J. Biol. Chem.* **288**, 11705-11717.

Esni, F., Ghosh, B., Biankin, A. V., Lin, J. W., Albert, M. A., Yu, X., MacDonald, R. J., Civin, C. I., Real, F. X., Pack, M. A. et al. (2004). Notch inhibits Ptf1 function and acinar cell differentiation in developing mouse and zebrafish pancreas. *Development* **131**, 4213-4224.

Gao, N., LeLay, J., Vatamaniuk, M. Z., Rieck, S., Friedman, J. R. and Kaestner, K. H. (2008). Dynamic regulation of Pdx1 enhancers by Foxa1 and Foxa2 is essential for pancreas development. *Genes Dev.* **22**, 3435-3448.

Ghosh, B. and Leach, S. D. (2006). Interactions between hairy/enhancer of split-related proteins and the pancreatic transcription factor Ptf1-p48 modulate function of the PTF1 transcriptional complex. *Biochem. J.* **393**, 679-685.

Golson, M. L., Loomes, K. M., Oakey, R. and Kaestner, K. H. (2009). Ductal malformation and pancreatitis in mice caused by conditional Jag1 deletion. *Gastroenterology* **136**, 1761-1771.e1.

Gong, Y., Ma, Z., Patel, V., Fischer, E., Hiesberger, T., Pontoglio, M. and Igarashi, P. (2009). HNF-1beta regulates transcription of the PKD modifier gene Kif12. *J. Am. Soc. Nephrol.* **20**, 41-47.

Gradwohl, G., Dierich, A., LeMeur, M. and Guillemot, F. (2000). neurogenin3 is required for the development of the four endocrine cell lineages of the pancreas. *Proc. Natl. Acad. Sci. USA* **97**, 1607-1611.

Gresh, L., Fischer, E., Reimann, A., Tanguy, M., Garbay, S., Shao, X., Hiesberger, T., Fiette, L., Igarashi, P., Yaniv, M. et al. (2004). A transcriptional network in polycystic kidney disease. *EMBO J.* **23**, 1657-1668.

Hald, J., Hjorth, J. P., German, M. S., Madsen, O. D., Serup, P. and Jensen, J. (2003). Activated Notch1 prevents differentiation of pancreatic acinar cells and attenuate endocrine development. *Dev. Biol.* **260**, 426-437.

Haldorsen, I. S., Vesterhus, M., Raeder, H., Jensen, D. K., Søvik, O., Molven, A. and Njølstad, P. R. (2008). Lack of pancreatic body and tail in HNF1B mutation carriers. *Diabet. Med.* **25**, 782-787.

Hale, M. A., Swift, G. H., Hoang, C. Q., Deering, T. G., Masui, T., Lee, Y.-K., Xue, J. and MacDonald, R. J. (2014). The nuclear hormone receptor family member NR5A2 controls aspects of multipotent progenitor cell formation and acinar differentiation during pancreatic organogenesis. *Development* **141**, 3123-3133.

Hart, A., Papadopoulou, S. and Edlund, H. (2003). Fgf10 maintains notch activation, stimulates proliferation, and blocks differentiation of pancreatic epithelial cells. *Dev. Dyn.* **228**, 185-193.

Haumaitre, C., Barbacci, E., Jenny, M., Ott, M. O., Gradwohl, G. and Cereghini, S. (2005). Lack of TCF2/vHNF1 in mice leads to pancreas agenesis. *Proc. Natl. Acad. Sci. USA* **102**, 1490-1495.

Haumaitre, C., Fabre, M., Cormier, S., Baumann, C., Delezoide, A.-L. and Cereghini, S. (2006). Severe pancreas hypoplasia and multicystic renal dysplasia in two human fetuses carrying novel HNF1beta/MODY5 mutations. *Hum. Mol. Genet.* **15**, 2363-2375.

Heliot, C. and Cereghini, S. (2012). Analysis of in vivo transcription factor recruitment by chromatin immunoprecipitation of mouse embryonic kidney. *Methods Mol. Biol.* **886**, 275-291.

Heliot, C., Desgrange, A., Buisson, I., Prunskaite-Hyyrylainen, R., Shan, J., Vainio, S., Umbhauer, M. and Cereghini, S. (2013). HNF1B controls proximal-intermediate nephron segment identity in vertebrates by regulating Notch signalling components and Irx1/2. *Development* **140**, 873-885.

Hiesberger, T., Shao, X., Gourley, E., Reimann, A., Pontoglio, M. and Igarashi, P. (2005). Role of the hepatocyte nuclear factor-1beta (HNF-1beta) C-terminal domain in Pkhd1 (ARPKD) gene transcription and renal cystogenesis. *J. Biol. Chem.* **280**, 10578-10586.

Ho, H. K., Pok, S., Streit, S., Ruhe, J. E., Hart, S., Lim, K. S., Loo, H. L., Aung, M. O., Lim, S. G. and Ullrich, A. (2009). Fibroblast growth factor receptor 4 regulates proliferation, anti-apoptosis and alpha-fetoprotein secretion during hepatocellular carcinoma progression and represents a potential target for therapeutic intervention. *J. Hepatol.* **50**, 118-127.

Hou, X., Mrug, M., Yoder, B. K., Lefkowitz, E. J., Kremmidiotis, G., D'Eustachio, P., Beier, D. R. and Guay-Woodford, L. M. (2002). Cystin, a novel cilia-associated protein, is disrupted in the cpk mouse model of polycystic kidney disease. *J. Clin. Invest.* **109**, 533-540.

Jacquemin, P., Durviaux, S. M., Jensen, J., Godfraind, C., Gradwohl, G., Guillemot, F., Madsen, O. D., Carmeliet, P., Dewerchin, M., Collen, D. et al. (2000). Transcription factor hepatocyte nuclear factor 6 regulates pancreatic endocrine cell differentiation and controls expression of the proendocrine gene ngn3. *Mol. Cell. Biol.* **20**, 4445-4454.

Jensen, J., Pedersen, E. E., Galante, P., Hald, J., Heller, R. S., Ishibashi, M., Kageyama, R., Guillemot, F., Serup, P. and Madsen, O. D. (2000). Control of endodermal endocrine development by Hes-1. *Nat. Genet.* **24**, 36-44.

Kaestner, K. H., Katz, J., Liu, Y., Drucker, D. J. and Schutz, G. (1999). Inactivation of the winged helix transcription factor HNF3alpha affects glucose homeostasis and islet glucagon gene expression in vivo. *Genes Dev.* **13**, 495-504.

Kang, H. S., Beak, J. Y., Kim, Y.-S., Herbert, R. and Jetten, A. M. (2009a). Glis3 is associated with primary cilia and Wwtr1/TAZ and implicated in polycystic kidney disease. *Mol. Cell. Biol.* **29**, 2556-2569.

Kang, H. S., Kim, Y.-S., ZeRuth, G., Beak, J. Y., Gerrish, K., Kilic, G., Sosa-Pineda, B., Jensen, J., Foley, J. and Jetten, A. M. (2009b). Transcription factor Glis3, a novel critical player in the regulation of pancreatic beta-cell development and insulin gene expression. *Mol. Cell. Biol.* **29**, 6366-6379.

Kim, Y.-S., Kang, H. S., Takeda, Y., Hom, L., Song, H.-Y., Jensen, J. and Jetten, A. M. (2012). Glis3 regulates neurogenin 3 expression in pancreatic beta-cells and interacts with its activator, Hnf6. *Mol. Cells* **34**, 193-200.

Kopp, J. L., Dubois, C. L., Schaffer, A. E., Hao, E., Shih, H. P., Seymour, P. A., Ma, J. and Sander, M. (2011). Sox9+ ductal cells are multipotent progenitors throughout development but do not produce new endocrine cells in the normal or injured adult pancreas. *Development* **138**, 653-665.

Kornfeld, J.-W., Baitzel, C., Könner, A. C., Nicholls, H. T., Vogt, M. C., Herrmanns, K., Scheja, L., Haumaitre, C., Wolf, A. M., Knippschild, U. et al. (2013). Obesity-induced overexpression of miR-802 impairs glucose metabolism through silencing of Hnf1b. *Nature* **494**, 111-115.

Lee, J. C., Smith, S. B., Watada, H., Lin, J., Scheel, D., Wang, J., Mirmira, R. G. and German, M. S. (2001). Regulation of the pancreatic pro-endocrine gene neurogenin3. *Diabetes* **50**, 928-936.

Lemaire, L. A., Goulley, J., Kim, Y. H., Carat, S., Jacquemin, P., Rougemont, J., Constam, D. B. and Grapin-Botton, A. (2015). Bicaudal C1 promotes pancreatic NEUROG3+ endocrine progenitor differentiation and ductal morphogenesis. *Development* **142**, 858-870.

Livak, K. J. and Schmittgen, T. D. (2001). Analysis of relative gene expression data using real-time quantitative PCR and the 2(-Delta Delta C(T)) method. *Methods* **25**, 402-408.

Lokmane, L., Haumaitre, C., Garcia-Villalba, P., Anselme, I., Schneider-Maunoury, S. and Cereghini, S. (2008). Crucial role of vHNF1 in vertebrate hepatic specification. *Development* **135**, 2777-2786.

Lynn, F. C., Smith, S. B., Wilson, M. E., Yang, K. Y., Nekrep, N. and German, M. S. (2007). Sox9 coordinates a transcriptional network in pancreatic progenitor cells. *Proc. Natl. Acad. Sci. USA* **104**, 10500-10505.

Maestro, M. A., Boj, S. F., Luco, R. F., Pierreux, C. E., Cabedo, J., Servitja, J. M., German, M. S., Rousseau, G. G., Lemaigre, F. P. and Ferrer, J. (2003). Hnf6 and Tcf2 (MODY5) are linked in a gene network operating in a precursor cell domain of the embryonic pancreas. *Hum. Mol. Genet.* **12**, 3307-3314.

Magenheim, J., Klein, A. M., Stanger, B. Z., Ashery-Padan, R., Sosa-Pineda, B., Gu, G. and Dor, Y. (2011). Ngn3(+) endocrine progenitor cells control the fate and morphogenesis of pancreatic ductal epithelium. *Dev. Biol.* **359**, 26-36.

Massa, F., Garbay, S., Bouvier, R., Sugitani, Y., Noda, T., Gubler, M.-C., Heidet, L., Pontoglio, M. and Fischer, E. (2013). Hepatocyte nuclear factor 1beta controls nephron tubular development. *Development* **140**, 886-896.

Miura, S., Mitsuhashi, N., Shimizu, H., Kimura, F., Yoshidome, H., Otsuka, M., Kato, A., Shida, T., Okamura, D. and Miyazaki, M. (2012). Fibroblast growth factor 19 expression correlates with tumor progression and poorer prognosis of hepatocellular carcinoma. *BMC Cancer* **12**, 56.

Mrug, M., Li, R., Cui, X., Schoeb, T. R., Churchill, G. A. and Guay-Woodford, L. M. (2005). Kinesin family member 12 is a candidate polycystic kidney disease modifier in the cpk mouse. *J. Am. Soc. Nephrol.* **16**, 905-916.

Murtaugh, L. C., Stanger, B. Z., Kwan, K. M. and Melton, D. A. (2003). Notch signaling controls multiple steps of pancreatic differentiation. *Proc. Natl. Acad. Sci. USA* **100**, 14920-14925.

Nammo, T., Yamagata, K., Tanaka, T., Kodama, T., Sladek, F. M., Fukui, K., Katsube, F., Sato, Y., Miyagawa, J.-i. and Shimomura, I. (2008). Expression of HNF-4alpha (MODY1), HNF-1beta (MODY5), and HNF-1alpha (MODY3) proteins in the developing mouse pancreas. *Gene Expr. Patterns* **8**, 96-106.

Oliver-Krasinski, J. M., Kasner, M. T., Yang, J., Crutchlow, M. F., Rustgi, A. K., Kaestner, K. H. and Stoffers, D. A. (2009). The diabetes gene Pdx1 regulates the transcriptional network of pancreatic endocrine progenitor cells in mice. *J. Clin. Invest.* **119**, 1888-1898.

Pan, F. C. and Wright, C. (2011). Pancreas organogenesis: from bud to plexus to gland. *Dev. Dyn.* **240**, 530-565.

Pierreux, C. E., Poll, A. V., Kemp, C. R., Clotman, F., Maestro, M. A., Cordi, S., Ferrer, J., Leyns, L., Rousseau, G. G. and Lemaigre, F. P. (2006). The transcription factor hepatocyte nuclear factor-6 controls the development of pancreatic ducts in the mouse. *Gastroenterology* **130**, 532-541.

Pin, C. L., Rukstalis, J. M., Johnson, C. and Konieczny, S. F. (2001). The bHLH transcription factor Mist1 is required to maintain exocrine pancreas cell organization and acinar cell identity. *J. Cell Biol.* **155**, 519-530.

Poll, A. V., Pierreux, C. E., Lokmane, L., Haumaitre, C., Achouri, Y., Jacquemin, P., Rousseau, G. G., Cereghini, S. and Lemaigre, F. P. (2006). A vHNF1/TCF2-HNF6 cascade regulates the transcription factor network that controls generation of pancreatic precursor cells. *Diabetes* **55**, 61-69.

Prevot, P.-P., Simion, A., Grimont, A., Colletti, M., Khalaileh, A., Van den Steen, G., Sempoux, C., Xu, X., Roelants, V., Hald, J. et al. (2012). Role of the ductal transcription factors HNF6 and Sox9 in pancreatic acinar-to-ductal metaplasia. *Gut* **61**, 1723-1732.

Pulkkinen, M.-A., Spencer-Dene, B., Dickson, C. and Otonkoski, T. (2003). The IIIb isoform of fibroblast growth factor receptor 2 is required for proper growth and branching of pancreatic ductal epithelium but not for differentiation of exocrine or endocrine cells. *Mech. Dev.* **120**, 167-175.

Raynaud, P., Tate, J., Callens, C., Cordi, S., Vandersmissen, P., Carpentier, R., Sempoux, C., Devuyst, O., Pierreux, C. E., Courtoy, P. et al. (2011). A classification of ductal plate malformations based on distinct pathogenic mechanisms of biliary dysmorphogenesis. *Hepatology* **53**, 1959-1966.

Rieck, S., Bankaitis, E. D. and Wright, C. V. E. (2012). Lineage determinants in early endocrine development. *Semin. Cell Dev. Biol.* **23**, 673-684.

Rooman, I., De Medts, N., Baeyens, L., Lardon, J., De Breuck, S., Heimberg, H. and Bouwens, L. (2006). Expression of the Notch signaling pathway and effect on exocrine cell proliferation in adult rat pancreas. *Am. J. Pathol.* **169**, 1206-1214.

Rovira, M., Scott, S.-G., Liss, A. S., Jensen, J., Thayer, S. P. and Leach, S. D. (2010). Isolation and characterization of centroacinar/terminal ductal progenitor cells in adult mouse pancreas. *Proc. Natl. Acad. Sci. USA* **107**, 75-80.

Rukstalis, J. M. and Habener, J. F. (2007). Snail2, a mediator of epithelial-mesenchymal transitions, expressed in progenitor cells of the developing endocrine pancreas. *Gene Expr. Patterns* **7**, 471-479.

Senkel, S., Lucas, B., Klein-Hitpass, L. and Ryffel, G. U. (2005). Identification of target genes of the transcription factor HNF1beta and HNF1alpha in a human embryonic kidney cell line. *Biochim. Biophys. Acta* **1731**, 179-190.

Seymour, P. A. and Sander, M. (2011). Historical perspective: beginnings of the beta-cell: current perspectives in beta-cell development. *Diabetes* **60**, 364-376.

Seymour, P. A., Freude, K. K., Tran, M. N., Mayes, E. E., Jensen, J., Kist, R., Scherer, G. and Sander, M. (2007). SOX9 is required for maintenance of the pancreatic progenitor cell pool. *Proc. Natl. Acad. Sci. USA* **104**, 1865-1870.

Seymour, P. A., Freude, K. K., Dubois, C. L., Shih, H.-P., Patel, N. A. and Sander, M. (2008). A dosage-dependent requirement for Sox9 in pancreatic endocrine cell formation. *Dev. Biol.* **323**, 19-30.

Seymour, P. A., Shih, H. P., Patel, N. A., Freude, K. K., Xie, R., Lim, C. J. and Sander, M. (2012). A Sox9/Fgf feed-forward loop maintains pancreatic organ identity. *Development* **139**, 3363-3372.

Shah, R. N. H., Ibbitt, J. C., Alitalo, K. and Hurst, H. C. (2002). FGFR4 overexpression in pancreatic cancer is mediated by an intronic enhancer activated by HNF1alpha. *Oncogene* **21**, 8251-8261.

Shi, G., Zhu, L., Sun, Y., Bettencourt, R., Damsz, B., Hruban, R. H. and Konieczny, S. F. (2009). Loss of the acinar-restricted transcription factor Mist1 accelerates Kras-induced pancreatic intraepithelial neoplasia. *Gastroenterology* **136**, 1368-1378.

Shih, D. Q., Navas, M. A., Kuwajima, S., Duncan, S. A. and Stoffel, M. (1999). Impaired glucose homeostasis and neonatal mortality in hepatocyte nuclear factor 3alpha-deficient mice. *Proc. Natl. Acad. Sci. USA* **96**, 10152-10157.

Shih, H. P., Kopp, J. L., Sandhu, M., Dubois, C. L., Seymour, P. A., Grapin-Botton, A. and Sander, M. (2012). A Notch-dependent molecular circuitry initiates pancreatic endocrine and ductal cell differentiation. *Development* **139**, 2488-2499.

Solar, M., Cardalda, C., Houbracken, I., Martín, M., Maestro, M. A., De Medts, N., Xu, X., Grau, V., Heimberg, H., Bouwens, L. et al. (2009). Pancreatic exocrine duct cells give rise to insulin-producing beta cells during embryogenesis but not after birth. *Dev. Cell* **17**, 849-860.

Stanger, B. Z., Tanaka, A. J. and Melton, D. A. (2007). Organ size is limited by the number of embryonic progenitor cells in the pancreas but not the liver. *Nature* **445**, 886-891.

Tao, B., Bu, S., Yang, Z., Siroky, B., Kappes, J. C., Kispert, A. and Guay-Woodford, L. M. (2009). Cystin localizes to primary cilia via membrane microdomains and a targeting motif. *J. Am. Soc. Nephrol.* **20**, 2570-2580.

Verdeguer, F., Le Corre, S., Fischer, E., Callens, C., Garbay, S., Doyen, A., Igarashi, P., Terzi, F. and Pontoglio, M. (2010). A mitotic transcriptional switch in polycystic kidney disease. *Nat. Med.* **16**, 106-110.

Ward, C. J., Hogan, M. C., Rossetti, S., Walker, D., Sneddon, T., Wang, X., Kubly, V., Cunningham, J. M., Bacallao, R., Ishibashi, M. et al. (2002). The gene mutated in autosomal recessive polycystic kidney disease encodes a large, receptor-like protein. *Nat. Genet.* **30**, 259-269.

Ware, S. M., Aygun, M. G. and Hildebrandt, F. (2011). Spectrum of clinical diseases caused by disorders of primary cilia. *Proc. Am. Thorac. Soc.* **8**, 444-450.

Weinstein, M., Xu, X., Ohyama, K. and Deng, C. X. (1998). FGFR-3 and FGFR-4 function cooperatively to direct alveogenesis in the murine lung. *Development* **125**, 3615-3623.

Wells, J. M., Esni, F., Boivin, G. P., Aronow, B. J., Stuart, W., Combs, C., Sklenka, A., Leach, S. D. and Lowy, A. M. (2007). Wnt/beta-catenin signaling is required for development of the exocrine pancreas. *BMC Dev. Biol.* **7**, 4.

Xuan, S., Borok, M. J., Decker, K. J., Battle, M. A., Duncan, S. A., Hale, M. A., Macdonald, R. J. and Sussel, L. (2012). Pancreas-specific deletion of mouse Gata4 and Gata6 causes pancreatic agenesis. *J. Clin. Invest.* **122**, 3516-3528.

Yang, Y., Chang, B. H.-J., Yechoor, V., Chen, W., Li, L., Tsai, M.-J. and Chan, L. (2011). The Krüppel-like zinc finger protein GLIS3 transactivates neurogenin 3 for proper fetal pancreatic islet differentiation in mice. *Diabetologia* **54**, 2595-2605.

Ye, Y. W., Zhou, Y., Yuan, L., Wang, C. M., Du, C. Y., Zhou, X. Y., Zheng, B. Q., Cao, X., Sun, M. H., Fu, H. et al. (2011). Fibroblast growth factor receptor 4 regulates proliferation and antiapoptosis during gastric cancer progression. *Cancer* **117**, 5304-5313.

Zhang, H., Ables, E. T., Pope, C. F., Washington, M. K., Hipkens, S., Means, A. L., Path, G., Seufert, J., Costa, R. H., Leiter, A. B. et al. (2009). Multiple, temporal-specific roles for HNF6 in pancreatic endocrine and ductal differentiation. *Mech. Dev.* **126**, 958-973.

Zhu, L., Tran, T., Rukstalis, J. M., Sun, P., Damsz, B. and Konieczny, S. F. (2004). Inhibition of Mist1 homodimer formation induces pancreatic acinar-to-ductal metaplasia. *Mol. Cell. Biol.* **24**, 2673-2681.

Supplemental Methods

Chromatin immunoprecipitation studies

E12.5 dissected WT pancreata were fixed in 1% formaldehyde at RT for 10 min and quenched with 125 mM glycine. Nuclei were lysed in RIPA buffer, flash-freezed in liquid nitrogen and kept at -80º C. Chromatin pools (n=150) were sonicated (15x 10sec ON / 1min30 OFF, Bioruptor UCD-200TM-EX) to obtain fragments of ~500bp, and then incubated overnight at 4º C with 4 μg of Hnf1b or rabbit IgG antibodies (both from Santa-Cruz).

The Hnf1b antibody (H85, Santa Cruz) was raised against a non-conserved domain between the dimerization domain and the POU specific domain of HNF1b and it does not cross react with HNF1a. It was extensively validated by immunoprecipitation, immunofluorescence and western blot techniques using WT and mutant tissues. Antibody specificity was further determined by the formation of specific supershifts on gel shif binding assays using either kidney extracts or extracts from transfected cells overexpressing Hnf1b or Hnf1a proteins. Furthermore, the ability of the antibody to react with endogenous Hnf1b protein in cross-linked chromatin was analyzed by ChIP on embryonic kidneys, assaying two well-known targets genes: Ksp-Cadherin and Wnt9 (first intron) (see Heliot and Cereghini, 2012; Heliot et al, 2013; Lokmane et al, 2010).

Chromatin-antibody complexes were immunoprecipitated with Protein-A agarose (Roche). Eluted chromatin was decrosslinked at 65ºC and purified by phenol/chloroform extraction. Immunoprecipitated chromatin and input (0.01% dilution) were analyzed by qPCR. These data were normalized to a reference DNA (pool of diluted inputs) and then expressed as fold enrichment relative to the values obtained with the immunoprecipitated chromatin using the non- immune IgG serum. A total of 4 targets were analyzed in duplicate per ChIP experiment, with at least 3 independent experiments performed for each of these targets.

Figure S1. No phenotypic difference between control and heterozygous pancreata. Haematoxylin/Eosin staining of control and heterozygous *Pdx1-Cre;Hnf1b*$^{+/Flox}$ pancreata at E16.5, showing no morphological difference in acinar, endocrine and ductal cells. Scale bars: 50 µm.

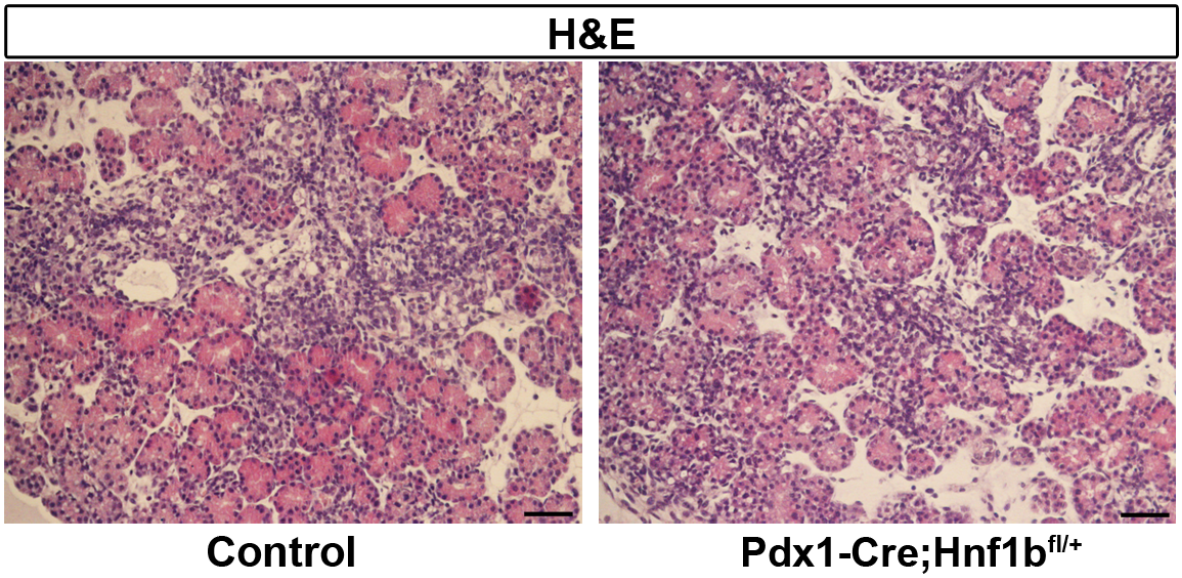

Figure S2. Pancreatic hypoplasia and morphogenesis defects in *Sox9-CreER^{T2};Hnf1b$^{Flox/LacZ}$* (TM E9.5) embryos.
(A, B) Digestive tracts of controls and *Sox9-CreER^{T2};Hnf1b$^{Flox/LacZ}$* (TM E9.5) mutants at E18.5 (C-F) Haematoxylin/Eosin staining of control and mutant pancreata at E16.5 and 18.5. Note the dramatic reduction in acinar cells in mutants (D, F) and cystic ducts (asterisks in F). (G) Pancreas weight of control, heterozygous (*Sox9-CreER^{T2};Hnf1b$^{Flox/+}$*) and mutant (*Sox9-CreER^{T2};Hnf1b$^{Flox/LacZ}$*) pancreata at E16.5 (TM at E9.5) (Control n=4, Heterozygous n=6, Mutant n=3), showing 40% decrease in mutants compared to controls. (H) qRT-PCR analysis of WT *Hnf1b* transcripts at E14.5 showing 70% decrease in *Hnf1b* expression in mutant pancreas (Control n=4, Mutant n=3). (I, J) Efficient *Hnf1b* inactivation in *Sox9-CreER^{T2};Hnf1b$^{Flox/LacZ}$;R26R$^{+/YFP}$* (TM E9.5) mutant pancreas at E11.5 shown by Hnf1b (red) and GFP (green) immunostainings. Note the high number of GFP+ cells with almost no Hnf1b+ cells in the mutant pancreas. Nuclei were stained in blue with DAPI. Scale bars: 200 µm in A-B; 50 µm in C-F and I-J'.

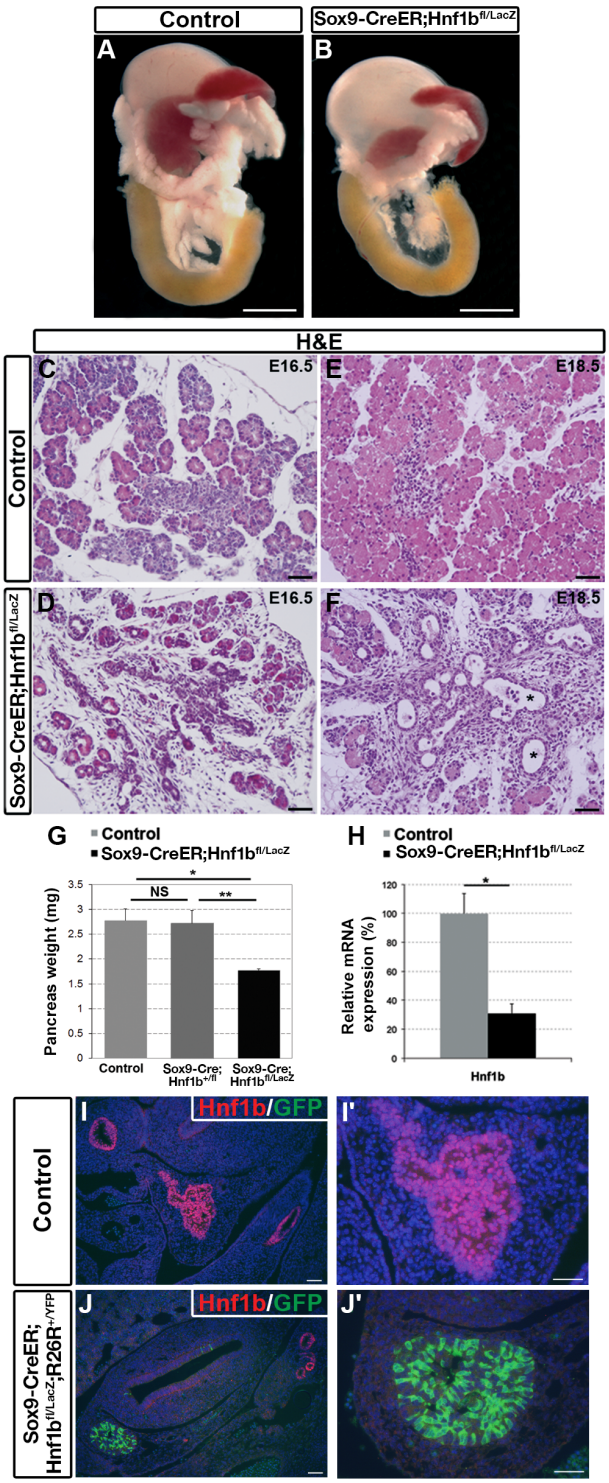

Figure S3. Lack of endocrine precursors in *Sox9-CreER^{T2};Hnf1b$^{Flox/LacZ}$* (TM E9.5) mutants.
(A, B) Amylase (AMY, green) and NGN3 (red) immunostainings in control and *Sox9-CreER^{T2};Hnf1b$^{Flox/LacZ}$* (TM E9.5) mutant pancreata at E16.5. Note the absence of Ngn3+ endocrine precursor cells in the mutant section (B). (C, D) Immunostainings of Insulin (INS, green) and Glucagon (GLUC, red) in control and *Sox9-CreER^{T2};Hnf1b$^{Flox/LacZ}$* (TM E9.5) mutant pancreata at E18.5. (E) qRT-PCR analysis of *Ngn3, Glucagon, Insulin, Somatostatin* and *Amylase* expression in controls and mutants at E16.5 (Control n=10, Mutant n=3). Scale bars: 50 µm.

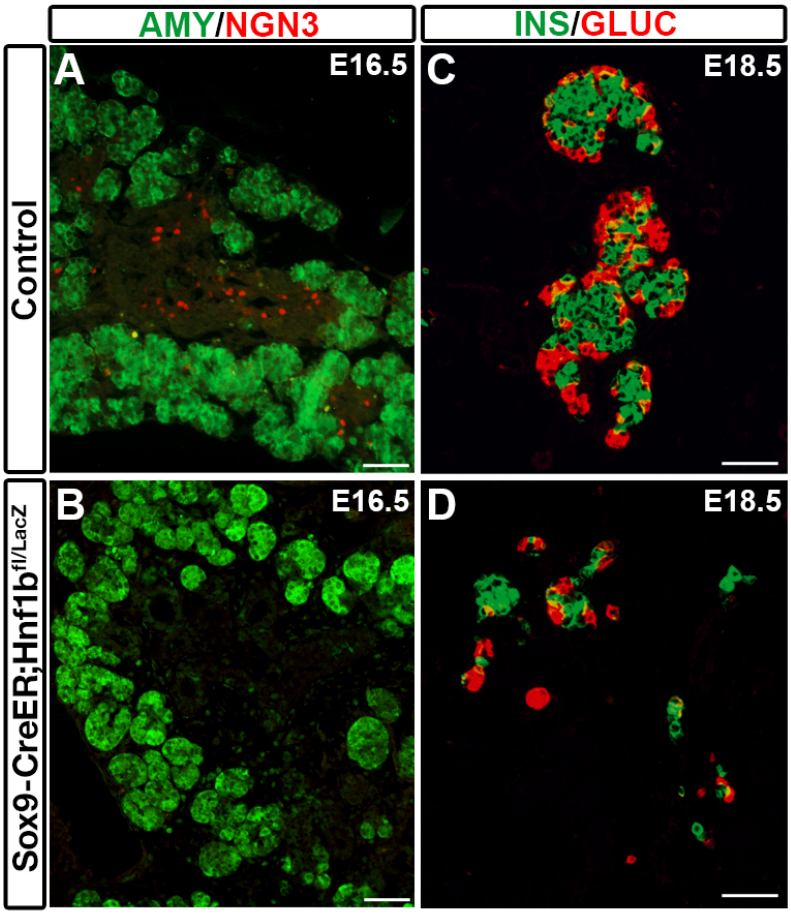

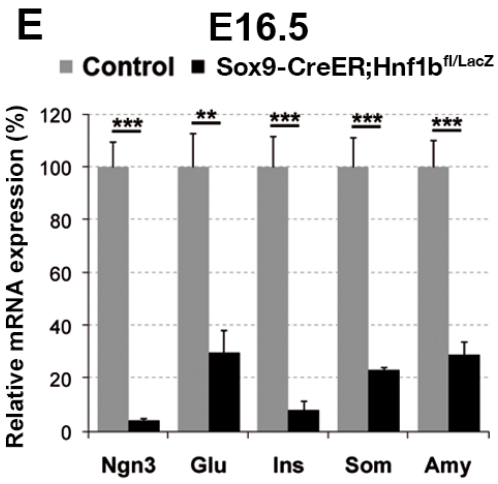

Figure S4. Cystic ducts with polarity defects in *Sox9-CreER^{T2};Hnf1b$^{Flox/LacZ}$* (TM E9.5) mutants.
(A, B) Sox9 immunohistochemistry of control and *Sox9-CreER^{T2};Hnf1b$^{Flox/LacZ}$* (TM E9.5) mutant pancreata at E18.5. (C, D) Mucin1 (MUC1, green) and β-catenin (red) coimmunostainings in control and *Sox9-CreER^{T2};Hnf1b$^{Flox/LacZ}$* (TM E9.5) mutant pancreata at E18.5. Note the polarity defects in epithelial cells lining the cysts, evidenced by a multilayered epithelium and a discontinuity in MUC1 expression at the apical region of ductal cells. Asterisks indicate cystic ducts in mutants (B, D). Scale bars: 50 µm.

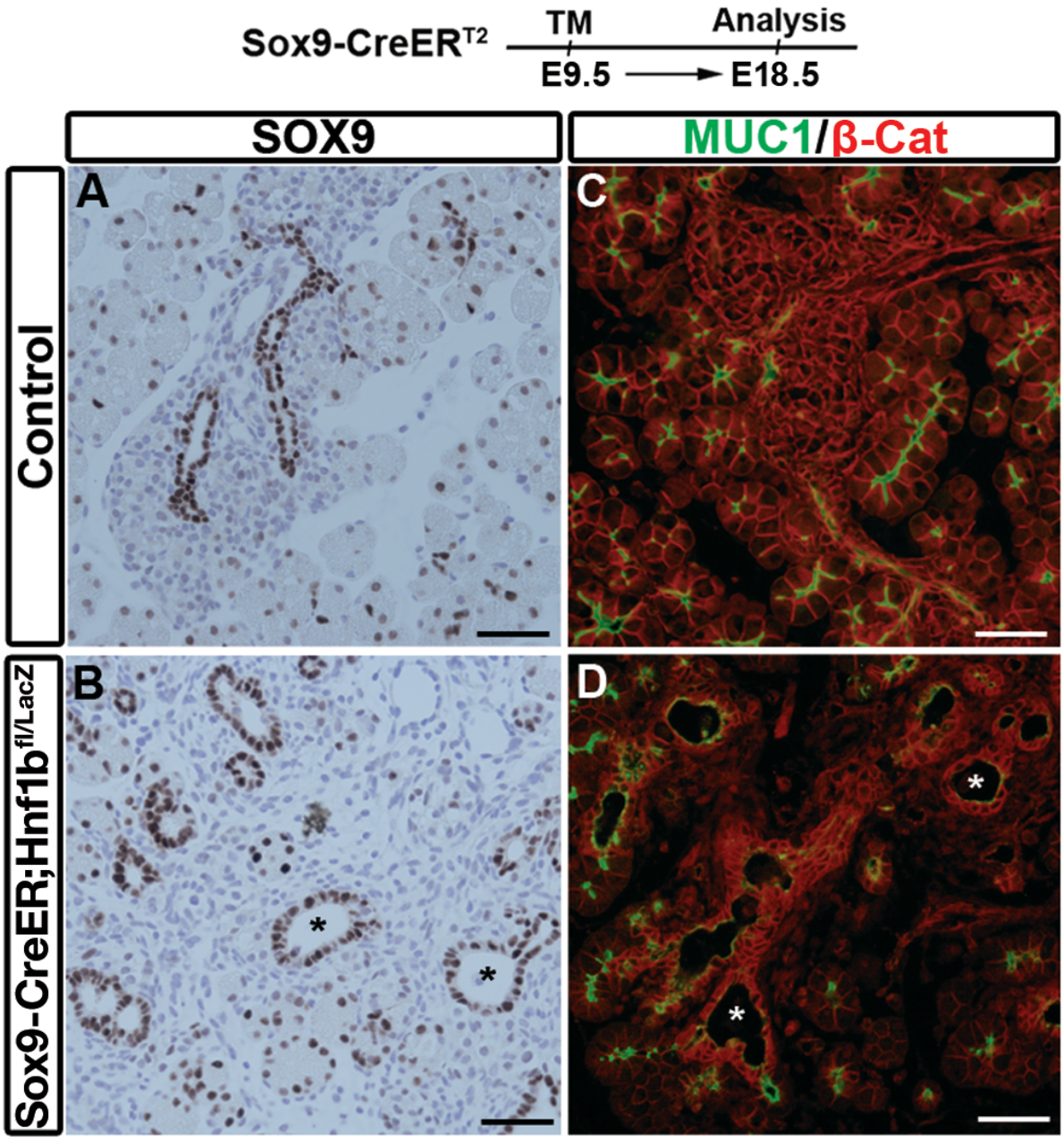

Figure S5. Exocrine defects in *Sox9-CreER^{T2};Hnf1b$^{Flox/LacZ}$* (TM E12.5) mutants.
(A) qRT-PCR analysis of the acinar markers *Ptf1a*, *Nr5a2*, *Mist1* and *Amylase* in control and *Sox9-CreER^{T2};Hnf1b$^{Flox/LacZ}$* (TM E12.5) mutant pancreata (Control n=8, Mutant n=7). (B-C) Amylase (AMY, green) staining showing a moderate loss of acinar cells in mutants. (D, E) MUC1 (green) and β-catenin (red) coimmunostainings showing cystic ducts and loss of polarity. Nuclei were stained in blue with DAPI. (I) qRT-PCR analysis of Notch pathway genes in control and *Sox9-CreER^{T2};Hnf1b$^{Flox/LacZ}$* (TM E12.5) at E16.5 (Control n=8, Mutant n=7), showing an upregulation of *Notch2, Hey2* and *Heyl* at the onset of acinar differentiation.

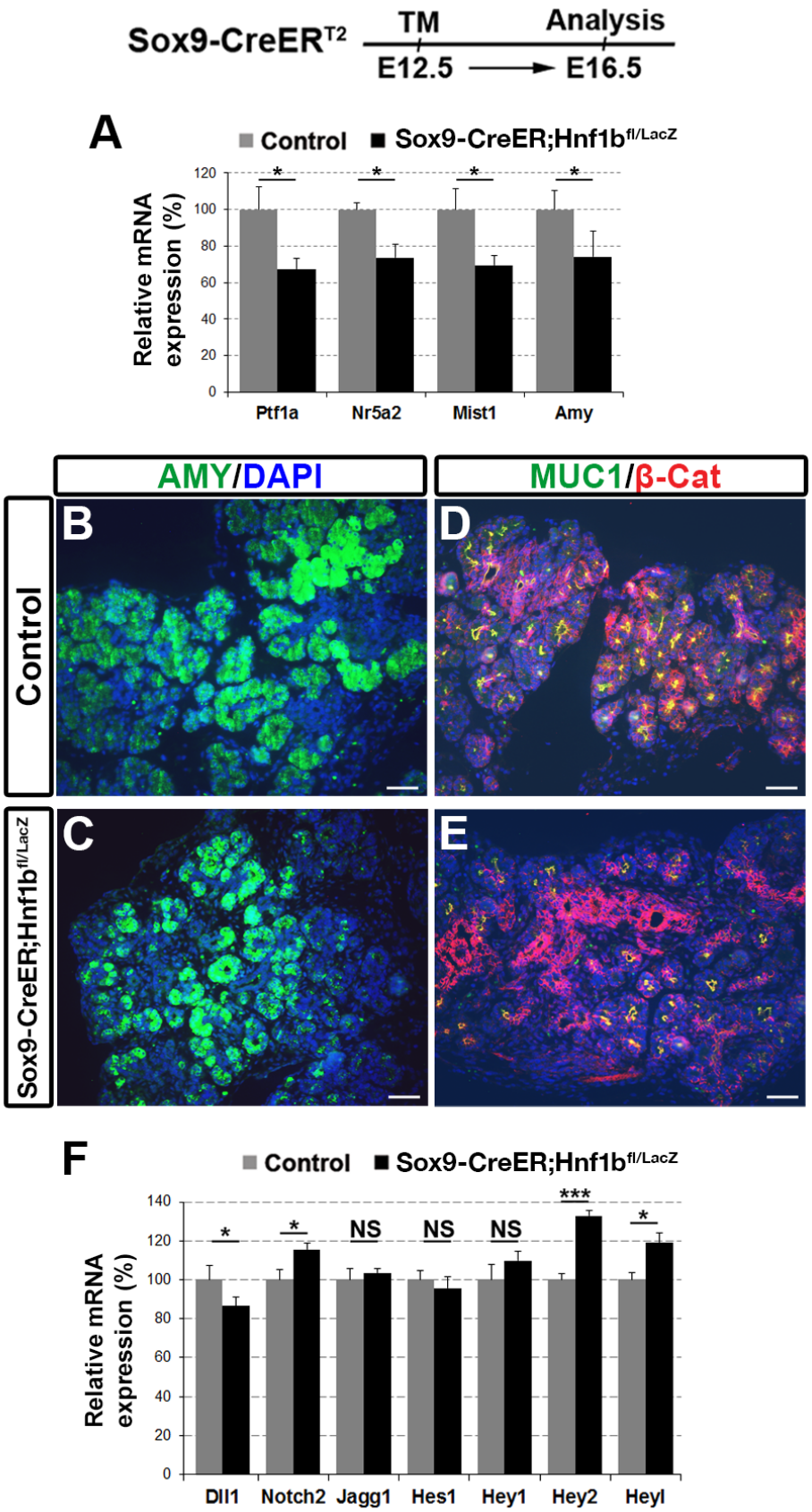

Figure S6. Regulatory sequences in *Ngn3* promoter.
Three regions upstream *Ngn3* TSS are represented: one distal (-5000 bp; -4740 bp), one intermediate (-4100 bp, -3200 bp) and one proximal (-900 bp; -170 bp). Putative binding sites for Hnf1b, Pdx1, Sox9 and FoxA2 were identified with the JASPAR database. Binding sites for Hnf6 were identified previously (Jacquemin et al., 2000). Sox9 binding sites could correspond to the ones previously described in the human promoter (-4061 bp; -3328 bp and –3306 bp; -400 bp and -385 bp; -161 bp upstream TSS) (Lynn et al., 2007). Intermediate regulatory sequences include the cluster 1 characterized in human (Lee et al., 2001). We identified 2 novel Hnf1b binding sites in the distal and the proximal regions, characterized by ChIP experiments (see Fig. 7). Hnf1b binding sites could correspond to putative ones in the human promoter identified by JASPAR database (-5043 bp, -3824 bp; -3783 bp; -445 bp).

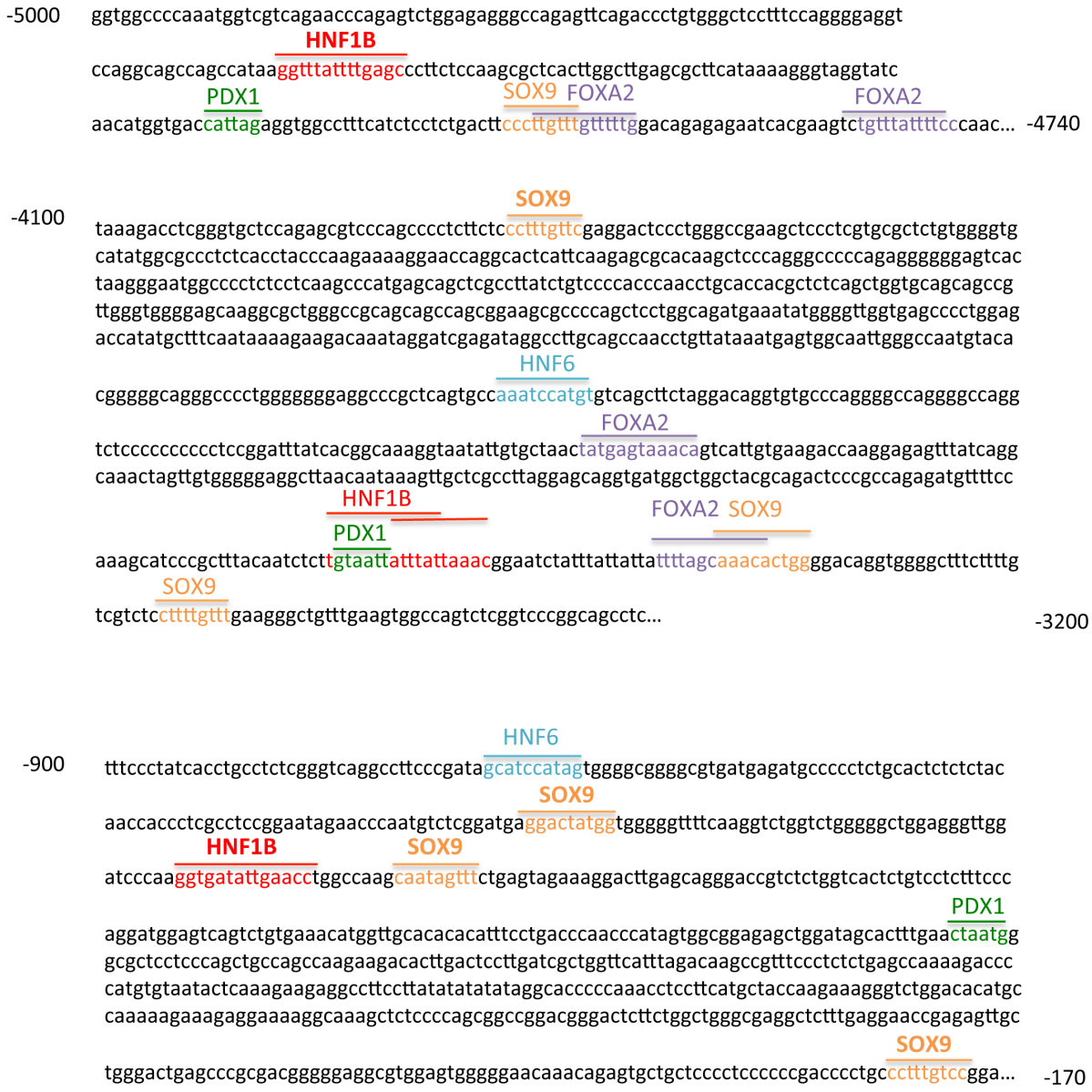

Table S1 : Primary and Secondary antibodies

Primary antibodies			
Antigen	**Host**	**Dilution**	**Source**
Hnf1b	rabbit	1/50	Santa Cruz
GFP	chicken	1/500	Aves Labs
P-Histone H3	mouse	1/300	Millipore
Pdx1	rabbit	1/1200	C. Wright,Vanderbilt University, USA
E-cadherin	mouse	1/100	BD Transd. Lab.
Ngn3	guinea pig	1/1000	M. Sander, University of California-San Diego, USA
CPA1	rabbit	1/500	Biogenesis
Insulin	rabbit	1/1000	ImmunoStar
Glucagon	mouse	1/1000	Sigma
Amylase	rabbit	1/300	Sigma
Sox9	rabbit	1/300	Chemicon
MUC1	Armenian hamster	1/100	Neomarkers
beta-Catenin	mouse	1/100	BD Transd. Lab.
acetylated alpha-Tubulin	mouse	1/300	Sigma
Hnf6	guinea pig	1/5000	P. Jacquemin & F. lemaigre, De Duve Institute, Belgium
pan-Cytokeratin	mouse	1/100	Sigma
Ezrin	rabbit	1/300	S. Louvet, UMR7622 CNRS UPMC, France
Dystroglycan	rabbit	1/200	Novus Biologicals
Laminin	rabbit	1/50	Sigma
AQP1	rabbit	1/100	Interchim
PKCz	rabbit	1/500	Sigma

Secondary antibodies			
Conjugation	**Species**	**Dilution**	**Source**
Cy3	rabbit	1/500	Jackson
Alexa Fluor 488	rabbit	1/500	Invitrogen
Alexa Fluor 488	mouse	1/500	Invitrogen
Alexa Fluor 488	chicken	1/500	Jackson
FITC	Armenian hamster	1/500	Jackson
Biotin	rabbit	1/1000	Vector
Streptavidin-Alexa 594	-	1/500	Jackson

Table S2. Oligonucleotide sequences for qRT-PCR and ChIP experiments.

qRT-PCR gene expression

Name	Forward Sequence (5'→3')	Reverse Sequence (5'→3')
Cyclophilin A	CAGGTCCTGGCATCTTGTCC	TTGCTGGTCTTGCCATTCCT
Hnf1b	GGCCTACGACCGGCAAAAGA	GGGAGACCCCTCGTTGCAAA
Sox9	AAGCCGACTCCCCACATTCCTC	CGCCCCTCTCGCTTCAGATCAA
Hnf6	CAAATCACCATCTCCCAGCAG	CAGACTCCTCCTCCTGGCATT
Ptf1a	TTCCTGAAGCACCTTTGACAGA	ACGGAGTTTCCTGGACAGAGT
Pdx1	CCAGATCTGCCTCTAGGACTCTTT	CAGTTTGGAGCCCAGGTTGT
Muc1	CTCTGGAAGACCCCAGCTCCAA	CCACGGAGCCTGACCTGAACT
Spp1	CCCTCCCGGTGAAAGTGACTGA	GCACCAGCCATGTGGCTATAGG
Mist1	TGGGCCTCCAGATCTCACCAA	CGTCACATGTCAGGTTTCTCTGCT
Nr5a2	CTGCTGGACTACACG GTTTGC	CTGCCTGCTTGCTGATTGC
Ck19	ACCCTCCCGAGATTACAACC	TCTGAAGTCATCTGCAGCCA
Pkhd1	TGCTCCTCAGGCAGGCAATCG	ACCTGTACCCTGGGGTGGCTT
Kif12	ACGAGGCTTCTATGTGGAACAG	GAGGTACCTGCTGAGAAGTTGG
Cys1	AGAGGAGCTCATGGCGAGCATT	GCCTGTGGCACAGATGCCAAGA
Glis3	TGGGAAGCCTCAGTTCCAGGTC	GCACTGAGGCCCAAAGCCAA
Bicc1	ACTCGGTGGAAGGCTGCAATGA	AGTCGCCAGCGTTTCCAGAATG
Pkd1	GCTGCATGCCAGTTCTTTTG	TTTTAAAGTGCAGAAGCCCCA
Pkd2	CATGTCTCGATGTGCCAAAGA	ATGGAGAACATTATGGTGAAGCC
Ngn3	TTCGCCCACAACTACATCTG	TTGGGAGACTGGGGAGTAGA
Glucagon	CCAAGAGGAACCGGAACAAC	CCTTCAGCATGCCTCTCAAAT
Insulin	ATCCACAATGCCACGCTTCT	AAACCCACCCAGGCTTTTGT
Somatostatin	TCCGTCAGTTTCTGCAGAAGTCTC	GTACTTGGCCAGTTCCTGTTTCCC
Amylase	CTGGGTTGATATTGCCAAGG	TGCACCTTGTCACCATGTCT
Notch1	AACACCGCCCGTGGATTCAT	ACATGTGGCACCCTCGAAGC
Notch2	CCTGCCAGGTTTTGAAGGGA	GGGCAGTCGTCGATATTCCG
Dll1	GCCCTCCATACAGACTCTCCC	AGGCGGCTGATGAGTCTTTCT
Jag1	TGCCCTCCAGGACATAGTGG	ACTCTCCCCATGGTGATGCA
Rbpj	GTTTTGGCGAGAGTTTGTGGAAGAT	TGGAGGCCGCTCACCAAACT
Lfng	CTCGCGCCACAAGGAGATGAC	CCGAGGAGCAGTTGGTGAGCA
Hes1	CAAAGACGGCCTCTGAGCAC	CCTTCGCCTCTTCTCCATGAT
Hes5	CTCCGCTCGCTAATCGCCTC	TCTCCACCGCCACGGTACTT
Hey1	TCACCTGAAAATGCTGCACAC	CGTGCGCGTCAAAATAACCT
Hey2	AGCGCCCTTGTGAGGAAACGA	TGTAGCGTGCCCAGGGTAATTG
Heyl	CAGCCCTTCGCAGATGCAA	CCAATCGTCGCAATTCAGAAAG
Fgfr2b	TGATGGGCTGCCCTACCTCAA	CCCCAGCATCCATCTCCGTCA
Fgfr4	CAGGCCTTCCACGGGGAGAAT	CACGGTCCGAGGGTACCACA

qPCR ChIP

Name *	# of HNF1B binding sites	Forward Sequence (5'→3')	Reverse Sequence (5'→3')	Amplicon genome location
Ngn3-700bp	1	TGGAGGGTTGGATCCCAAGGTG	CAGAGACGGTCCCTGCTCAAGT	chr10:61,595,110-61,595,193
Ngn3-3300bp	1	GGGGACAGGTGGGGCTTTCTT	GGGACCGAGACTGGCCACTT	chr10:61,592,554-61,592,627
Ngn3-4900bp	1	GGCCCCAAATGGTCGTCAGAAC	CAAGCCAAGTGAGCGCTTGGA	chr10:61,590,840-61,590,975
Hnf6+4950bp	2	CTTGCAGCTTGGTTGATTGA	CGGCAGTACCAGACACTTGA	chr9:74714652-74714752
Cys1-4500bp	4	TGATGGGAGTGTCCCGTGCAA	CATGGCTGGCTGTGTGCAGAA	chr12:25,371,128-25,371,227
Pkhd1-70bp	1	TCCTGTTGGACTGGAACTCA	AGCCCTTTCTTTGGGTCTCT	chr1:20,608,118-20,608,248
Glis3+120100bp	2	CAACAAGAAGCCCTTTTGGA	CATGTCAGAGATGAGGGAGGT	chr19:28,634,413-28,634,533
Fgfr4+280bp	2	AGCGCACACAGGGCCTTT	GCCCCGGTGGGCAATAAGT	chr13:55,254,476-55,254,555
Bicc1+2857	1	CCCCCAGGACAGTCTCTCTAAAA	TGGCCTTCAAGTCTTCAGAGTG	chr10:71,156,782-71,156,857

** Primer names indicate the approximate position of the HNF1B-binding site/s amplified, relative to the TSS of the respective gene.*